Science and Engineering Research Council
Rutherford Appleton Laboratory
Chilton DIDCOT Oxon OX11 0QX

RAL-90-011

laser

Oscillator and System Development on the Vulcan Glass Laser System for the Plasma Beat-Wave Program

C N Danson

N →

March 1990

OSCILLATOR AND SYSTEM DEVELOPMENT
ON THE
VULCAN GLASS LASER SYSTEM
FOR THE
PLASMA BEAT - WAVE PROGRAM

COLIN NICHOLAS DANSON

N.

This report was first submitted as a thesis for the degree of
Master of Philosophy to the CNAA, in January 1990,
in partial fulfilment of the requirements for the degree.

Sponsoring establishment : Newcastle upon Tyne Polytechnic
Collaborating establishment : The Rutherford Appleton Laboratory

OSCILLATOR AND SYSTEM DEVELOPMENT ON THE VULCAN GLASS LASER SYSTEM FOR THE PLASMA BEAT - WAVE PROGRAM

COLIN NICHOLAS DANSON

ABSTRACT

This thesis describes the oscillator and system development on the VULCAN glass laser undertaken in support of the RAL Plasma Beat-wave experiments. This program seeks to evaluate advanced particle acceleration schemes for a new generation of machines for fundamental research in high energy physics.

The experiments required two synchronised high power laser pulses of slightly different wavelength. These pulses were generated using two different laser media; Nd:YAG and Nd:YLF operating at 1.064 and 1.053 microns respectively. The first oscillator system developed operated with both lasing media housed in the same laser cavity. Problems with the stability of the optical output required the development of a second system which housed the two lasing media in separate cavities.

The second aspect of the development work, described in this thesis, was the reconfiguration of the VULCAN glass laser system to amplify the two laser pulses to power levels of 0.5 TW per pulse. The first scheduled experiment required the two pulses to be propagated co-linearly. To amplify the pulses to the high output powers required ywo amplifying media to be used which preferentially amplify the two lasing wavelengths. For the later experiments the two laser pulses were amplified in separate amplifier chains which required the design of an efficient beam combiner.

CONTENTS

ACKNOWLEDGEMENTS

I wish to thank my supervisers, Dr. G Evans and Dr. CB Edwards, and Dr. PT Rumsby for their help and encouragement throughout this project. I would also like to thank the Rutherford Appleton Laboratory and Newcastle-upon-Tyne Polytechnic for allowing me the opportunity to undertake this program of work.

I am grateful to Dr. AE Dangor, Dr. A Dymoke-Bradshaw, Dr. RG Evans and Dr. A Dyson for their enthusiasm in experimental Beat-wave research which has stimulated this and other programs and for useful discussions over the period.

I would also like to thank the staff at RAL within the VULCAN operations group for help with this work. In particular Mr. RWW Wyatt for his assistance and expertise in electronics and Mr. R Bann and Mrs. J Smith for their assistance in the preparation of this thesis.

I am also grateful to JK Lasers Ltd (now Lumonics Ltd), in particular Mr K Ure, for the loan of equipment which ensured that the project got started.

Finally I would like to thank all others who have helped in any way with this project.

CHAPTER 1.

Background.

Abstract

In this chapter a brief history of the laser is presented together with the growth of high power Nd:glass laser systems. The development of laser materials associated with neodymium lasers is also described as these materials feature in the development work on the Beat-wave driver described in Chapters 3 and 4.

1.1 The Birth of the Laser

The first laser was demonstrated in May 1960, resulting from post World War 2 developments of the Maser (Microwave Amplification by the Stimulated Emission of Radiation). The Maser was developed predominatly in the USA and the USSR resulting in Basov, Prokhorov and Townes sharing the 1964 Nobel Prize in Physics for their development work.

Throughout the 1950's physicists were looking for methods of amplifying stimulated emission at shorter wavelengths. In the USSR Fabrikant (1.1) and in the USA Dicke (1.2) filed patents on the principles of lasers and for the possibilities of using a Fabry-Perot interferometer as a resonant cavity. In the USSR Basov and Prokhorov proposed schemes based on an extension of the Maser principle at shorter wavelengths in the late 1950's, although it was a paper by Schawlow and Townes (1.3) published in 1958, which detailed the construction of an "optical maser", that is generally regarded as the invention of the laser. Javan (1.4) and Sanders (1.5) also discussed the possibilities of using electron excitation of gases.

Gordon Gould, in the USA, was also one of the early laser pioneers, but instead of publishing his ideas in 1957 had his notebooks notarised in the hope of obtaining a

patent in due course. It was he who defined the term LASER as the Light Amplification by the Stimulated Emission of Radiation. He eventually obtained two patents on the optical pumping of laser media and on more general laser applications. These patents have been the subject of intense legal proceedings but are currently still in force.

A number of different groups were working on developing the first operational laser. In May 1960 Maiman at the Hughes Research Laboratories was successful. He used a polished cube of ruby pumped by a helical flashlamp and obtained enhanced output and narrowing, consistent with stimulated emission, on the 694.3 nm line. The work was submitted to Physical Review Letters but was rejected as being " just another Maser paper ". The material was then accepted by Nature and was published in August 1960 (1.6).

The next couple of years saw a proliferation of different materials exhibiting laser action operating at different wavelengths. Those of note include the first demonstration of the HeNe laser in 1960 (1.7) and the first Carbon Dioxide laser in 1963 (1.8). With importance to this work the first Neodymium laser was demonstrated in 1961 (1.9) in a calcium-tungstate host and in the same year the first Nd:glass was demonstrated by Snitzer (1.10). It was in 1964 that the first Nd:YAG laser was demonstrated at the Bell Labs (1.11) producing an optical output at 1.064 microns.

With the development of the laser it was necessary to develop pulse control techniques to increase the energy and the power in the optical output. The first pulse amplifier was demonstrated by Kisliuk and Boyd (1.12) in 1961. The first Q-switching was developed by Hellwarth and McClung (1.13) in 1961 using mechanical and electro-optic techniques. This allowed the generation of high peak powers and nanosecond pulses, increasing the applications of the laser. To reduce the pulsewidth still further into the picosecond regime mode-locking techniques were developed in the middle 1960's. The first mode-locking was observed by Hargrove et al (1.14) in 1964 using an acousto-optic crystal in the

cavity of a HeNe laser. The first solid state mode-locking was achieved in 1965 by Deutsch (1.15) using an electro-optic Pockel cell in a ruby cavity.
A more comprehensive review of the history of the laser can be found in references 1.16 and 1.17.

1.2 Applications of High Power Laser Systems

With an intense laser beam it was proposed that it would be possible to use lasers as weapons and for the generation of fusion energy. These applications therefore provided the funding for large laser system development both for civil and military applications. The military application, other than as direct weapons systems, was to provide a relatively inexpensive means of studying weapons physics. For civil applications the appeal was the prospect of a "clean" fusion energy source. It was believed this could be achieved using the outputs of a multi-beam laser system to compress a pellet containing Deuterium / Tritium fuel, commonly called Inertial Confinement Fusion (ICF).
In the USA, because of the commitment to the technology and the large funding available, decisions concerning large system development have dictated world-wide development. In 1964 the US suspended work on large Neodymium laser systems in favour of Carbon Dioxide lasers operating at 10.6 microns. Later the experimental requirements for the ICF program shifted towards shorter wavelengths, leading to Nd:Glass being reconsidered in the early 1970's.

1.3 The Development of Nd:Glass Laser Materials

All the early solid-state systems operated with Nd:YAG oscillators (operating at 1.064 microns) with subsequent amplification in silicate glass amplifier chains. A comparison of some of the relevant lasing and thermal properties are shown in Table 1. As can be seen from the table the advantages of using Nd:YAG rather than

OPTICAL / THERMAL PROPERTIES	Nd : DOPED LASER HOST			
	SILICATE	PHOSPHATE	Nd:YAG	Nd:YLF
Refractive Index (n)	1.561	1.508	1.82	1.45
Non Linear Refractive Index, n_2($x10^{-13}$esu)	1.6	1.02	3.2	0.6
Lasing Wavelength (nm)	1061	1053.5	1064	1047/1053
Linewidth (nm [GHz])	278 [7,500]	196 [5,288]	6 [180]	12 [360]
Spontaneous Lifetime (s x 10^{-6})	350+	350+	240-270	450-570
Total Cross Section (x 10^{-19} cm^2)	0.27	0.42	6.5	1.9-2.3
Thermal Conductivity (W / m°K)	1.35	0.67	11	5
Thermo-Optic Effect dn/dt (ppm / °C)	8.1	0.4	7.3	-3
Expansion Coefficient (ppm / °C)	9.3	12.5	7.8	10
Damage Threshold (J / cm^2)	10+	10+	10+	10+

Information Sources : Koechner - Solid State Laser Engineering - Chapter 2
LLNL Annual Report 1978
Lasers and Applications
Schott Laser Glass Catalogue

COMPARISON OF NEODYMIUM LASER HOSTS
TABLE 1

silicate Nd:glass are its higher stimulated emission cross section, giving higher gain for the same pumping, and its higher thermal conductivity allowing heat to be dissipated efficiently from the rod. Unfortunately it is impossible to grow very large Nd:YAG crystals and therefore it is necessary to use glass hosts on any amplifier with a diameter larger than a few millimeters.

In the late 1970's progress in laser glass developments led to the introduction of phosphate glasses. The properties of phosphate glasses are summarised in Table 1. Compared with silicate glasses these had a higher stimulated emission cross section and a relatively small non-linear refractive index making them ideal for short-pulse amplification. The absolute limit of short pulse amplification is dictated by non-linear beam break-up which is dependent on the non-linear refractive index (detailed in Chapter 4). Another important advantage of phosphate glass hosts is that they have a very low thermo-optic constant, giving much lower refractive index gradients in the amplifier than in silicates. These gradients produce a thermal lensing of the beam passing through the rod, which affect the collimation of the beam, leading to problems in alignment (detailed in Chapter 4).

The peak gain for the phosphate glass is at $1.053 \pm .001$ microns. To drive the amplifier close to line centre requires a suitable oscillator. In 1976 Nd:YAG was operated at 1.052 microns, a lasing line having a much higher lasing threshold than the 1.064 micron line, therefore large spectral discrimination was required to suppress the preferred line. In 1978 phosphate glass oscillators were operated at 1.054 microns and in the same year Nd:YLF oscillators were revived operating at 1.053 microns (Nd:YLF first lased in the late 60's but problems in crystal growth made it unattractive compared to Nd:YAG). Glass laser hosts are not a preferred medium in oscillators because of their poor thermal conductivity. This leads to thermally induced birefringence producing a non-uniform spatial beam profile.

Nd:YLF is a uniaxial crystal, therefore the preferred stimulated line is dependent on the polarisation of the input beam. Using an intra-cavity polariser it is therefore possible to select either the 1.047 micron or the 1.053 micron line. The properties of

Nd:YLF are also presented in Table 1. The material has several properties which make it attractive compared to Nd:YAG: Its linewidth is twice that of Nd:YAG allowing for the generation of shorter pulses; It has a much lower non-linear refractive index; and a much lower thermo-optic constant reducing any problems associated with thermal lensing.

For the reasons given above when operating a large aperture system with short pulses at high output fluences a Nd:YLF/Phosphate glass combination is preferred over a Nd:YAG/Silicate combination.

1.4 The Growth of Nd:Glass Laser Systems

Applications at the various laboratories have dictated laser system development. Until very recently the applications have been dominated by ICF and weapon simulation. The applications are now more diverse, for example X-ray laser development and materials processing. As experimental requirements have changed and diagnostic techniques have become more refined the demands for more sophisticated laser systems has increased. This has led to the need for synchronised oscillator systems operating with complex pulse shapes to drive both the main experimental beams and auxiliary beams to diagnose the experiment.

Some of the different glass laser systems operated throughout the world since the early seventies are shown in Table 2. The table shows the rapid growth in output energies by over three orders of magnitude in only ten years of system developments. This is largely due to the ability to produce large laser optics. At the Lawrence Livermore National Laboratories (LLNL) in the USA the Janus system had output beams of 5 cm beam diameter whilst Nova has beam diameters of 76 cm. This has required the development of mirrors, for example, with flatness specifications of 0.25 microns over the full 1 metre aperture.

LASER SYSTEM	LOCATION	DATE	IR ENERGY	BEAMS
GEKKO - 1	OSAKA	1969	10 J	1
JANUS	LLNL	1974	10 J	1
GEKKO - II	OSAKA	1975	200 J	2
CYCLOPS	LLNL	1976	100 J	1
ARGUS	LLNL	1977	1 KJ	2
GEKKO - IV	OSAKA	1978	1 KJ	6
OMEGA	LLE	1978	4 KJ	24
SHIVA	LLNL	1978	10 KJ	20
NOVETTE	LLNL	1982	20 KJ	2
GEKKO - XII	OSAKA	1983	20 KJ	12
NOVA	LLNL	1984	100 KJ	10

THE GROWTH OF Nd:GLASS LASER SYSTEMS
TABLE 2

CHAPTER 2.

Introduction.

Abstract

This chapter describes the activities of the Central Laser Facilities and describes the VULCAN glass laser system. An introduction to the Beat-wave concept is presented together with the aims of the experiment.

2.1 The Central Laser Facilities

The VULCAN Nd:glass laser system is situated at the Rutherford Appleton Laboratory (RAL), in Oxfordshire which is the main establishment operated by the Science and Engineering Research Council (SERC). The SERC was set up to administer the distribution of funds for research in higher education and to provide central facilities to enable that research to be carried out. Those facilities managed by the Science Board include The Synchrotron Radiation Source at The Daresbury laboratory, the ISIS neutron source and the Central Laser Facilities (CLF), both at RAL. The SERC is also involved in international collaborative projects such as with the particle accelerators at CERN.

The CLF was established in 1975 with the remit to study laser generated dense plasmas and non-linear interactions of laser radiation with matter. The CLF was also to develop more efficient and new lasers for these and other purposes. In 1976 the first laser was installed. This consisted of a single chain of Nd:glass rod amplifiers delivering up to 10 Joules in a 100 ps pulse (100 GW). Over the next 13 years the VULCAN Nd:glass facility has been enhanced to the present level which consists of a multi-beam system capable of delivering 2.8 kJ in 1 ns or 6 TW in 100 ps.

In parallel with the glass laser development, a program of research and development on high power gas lasers has been pursued. In 1982 SPRITE; the worlds highest power KrF excimer laser, was capable of delivering 200 J in 60 ns at a wavelength of 249 nm. This laser as well as being a user facility has been used for development which has demonstrated Raman beam amplification and picosecond pulse generation. These developments will lead to the construction of multi-kJ short pulse systems in the mid 1990's.

Another important aspect of the work of the CLF is for the provision of ultra-short pulse, tunable systems. A number of different lasers are now available to user groups with applications predominantly in biology and chemistry.

2.2 The VULCAN Laser Facility

2.2.a Experimental Capabilities

The VULCAN Nd:glass laser has developed into an extremely versatile user facility, with diverse experimental configurations. In addition to the original experimental goals, other fields of current interest include x-ray lasers, x-ray microscopy, astro-physics applications, shock-waves and beat-wave accelerators. The uniquely versatile nature of the facility has attracted international collaboration on many experiments, with RAL hosting collaborative teams from Japan, the USA, Canada, the Soviet Union, France and China.

To cater for the wide range of experiments the facility has four independent target areas. Target Area West provides a vacuum chamber most suitable for twelve beam implosion experiments (ICF studies). Target Area East has two main configurations suitable for x-ray laser experiments and cluster beam interactions. Target Area Two can use only three of the VULCAN output beams but is designed for high versatility allowing a range of experiments to be conducted including the Beat-wave experiment. A fourth target area is available which only uses a single low

power beam, suitable for x-ray microscopy experiments and for instrumentation development.

2.2.b The Laser System

Any three of the target areas can be operational at one time. Each may require different system configurations in terms of pulse-widths and the number of beams on target. The laser is therefore designed to be flexible to meet the short and long term needs of the users, and is constantly modified to cater for new requirements. The authors role is to manage a small team of scientists and engineers to maintain and enhance the VULCAN laser facilities, with particular responsibilities for oscillator development.

The laser system can be divided into three readily identifiable stages.

(i) Pulse Generation

The pulse generation stage consists of a number of oscillators which produce the various pulses suitable for the experiments. The "standard" generators consist of a pair of synchronised long and short pulse oscillators. The short pulse oscillator uses a Nd:YLF rod and is actively mode-locked and Q-switched producing pulses of 70 - 300 ps in duration. The long pulse Nd:YLF oscillator operates with a single longitudinal mode producing an approximately gaussian 25 ns FWHM output. From this envelope a pulse of 0.5 - 10 ns can be switched using a chain of Pockel cells. Due to the design of the switchout system the two oscillator outputs are synchronised allowing one to be used as a driver pulse for the experiment and the other as a diagnostic.

There are three other oscillators which are used for specific experiments. An active / passive mode-locked Nd:YLF oscillator generates 20 - 30 ps pulses which cannot be synchronised to the other oscillator outputs. A broadband Nd:glass oscillator

generates nanosecond pulses for use in smoothing experiments. The third oscillator is the subject of this study and is described in detail in Chapter 3.

(ii) Rod Amplification

The pulses once generated are then amplified in two separate rod amplifier chains. An amplifier consists of a rod of Nd:glass surrounded by flashlamps. Water cooling of the amplifier allows it to be pulsed on a two minute cycle. The first amplifiers in the chain have a clear aperture of 9 mm. As the energy in the beam increases the beam diameter is expanded to prevent damage to optical components. The clear aperture of the rods also expand up to the last rod amplifier in the chain which has a clear aperture of 45 mm. The energy at the output of the rod amplifier chains in the short pulse is typically 2 J, while in the long pulse it is typically 10 J.
The beams at the output of the rods can be directed into either the six beam system or a single diagnostic beam line. Mirrors on kinematic mounts can be inserted to send a pulse down the appropriate beam line. Plate 1 shows a view of the laser from the output of the rod chains. In the top/centre of the picture are the protective covers over the oscillators can be clearly seen, with two of the insertable mirrors in the foreground.

(iii) Disc Amplification

Following the corner split the beams are expanded to 100 mm in diameter, and then amplified in double-pass disc amplifiers. The amplifiers consist of a series of six slabs of Nd:glass mounted at Brewster's angle relative to the beam. It is necessary to utilise this design of amplifier as it is impossible to achieve high gain with spatially uniform profiles from rod amplifiers at large apertures. This is because rod amplifiers use radial pumping. At high doping concentrations the gain will be radially non-uniform, with little pump radiation reaching the centre of the rod. The

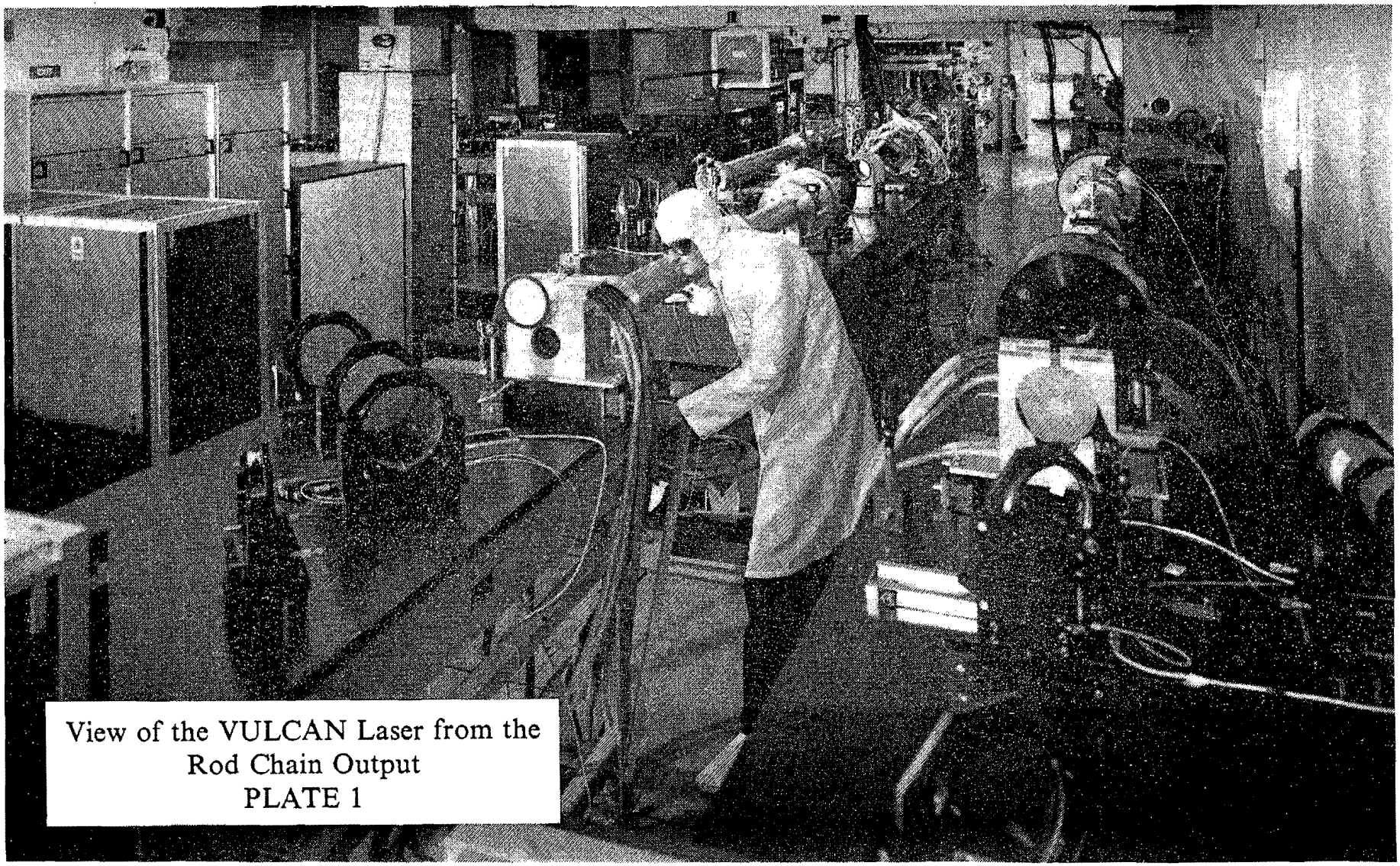

View of the VULCAN Laser from the Rod Chain Output
PLATE 1

disc amplifiers overcome this by pumping the Brewster surfaces of the slabs.
Plate 2 shows a view of the laser from the output of the disc amplifier stages. A single beam enters the room and is divided six ways. The beams are then amplified in the six disc amplifiers which dominate the picture. To the left of the Plate the single beam disc is visible. In the foreground are two of the 169 mm diameter mirrors which direct the beam along the appropriate path. The mirrors appear transmitting but are multi-layer dielectrics and hence are only high-reflecting at 1 micron.

System Output

At the output of the system each of the beams contains up to 300 J in 1 ns pulses or 0.5 TW in 100 ps pulses. Using a series of kinematically mounted insertable mirrors the beams can be directed to the three main target areas.

2.3 The Beat-Wave Accelerator Concept.

The first accelerator was built by Cockroft and Walton at the Cavendish Laboratories in 1932. Since then there has been an exponential increase in energy available to experiments from a variety of accelerator designs. Circular accelerators are adequate for proton acceleration to energies in excess of 20-TeV. For electrons, energy losses due to synchrotron radiation force the use of linear accelerators. For example at 1 TeV an electron in the 50 mile circumference Superconducting Super Collider (SSC) in the USA would lose half its energy in one revolution. Therefore it is necessary to use linear colliders for electron acceleration.
With current technology it is possible to produce an accelerating gradient of 17 megavolts per meter using the two-mile-long Stanford Linear Collider producing 100 GeV e + e- collisions. This is state of the art for rf linacs, where the accelerating gradient is limited by electrical break-down. To obtain 1 TeV linear colliders would

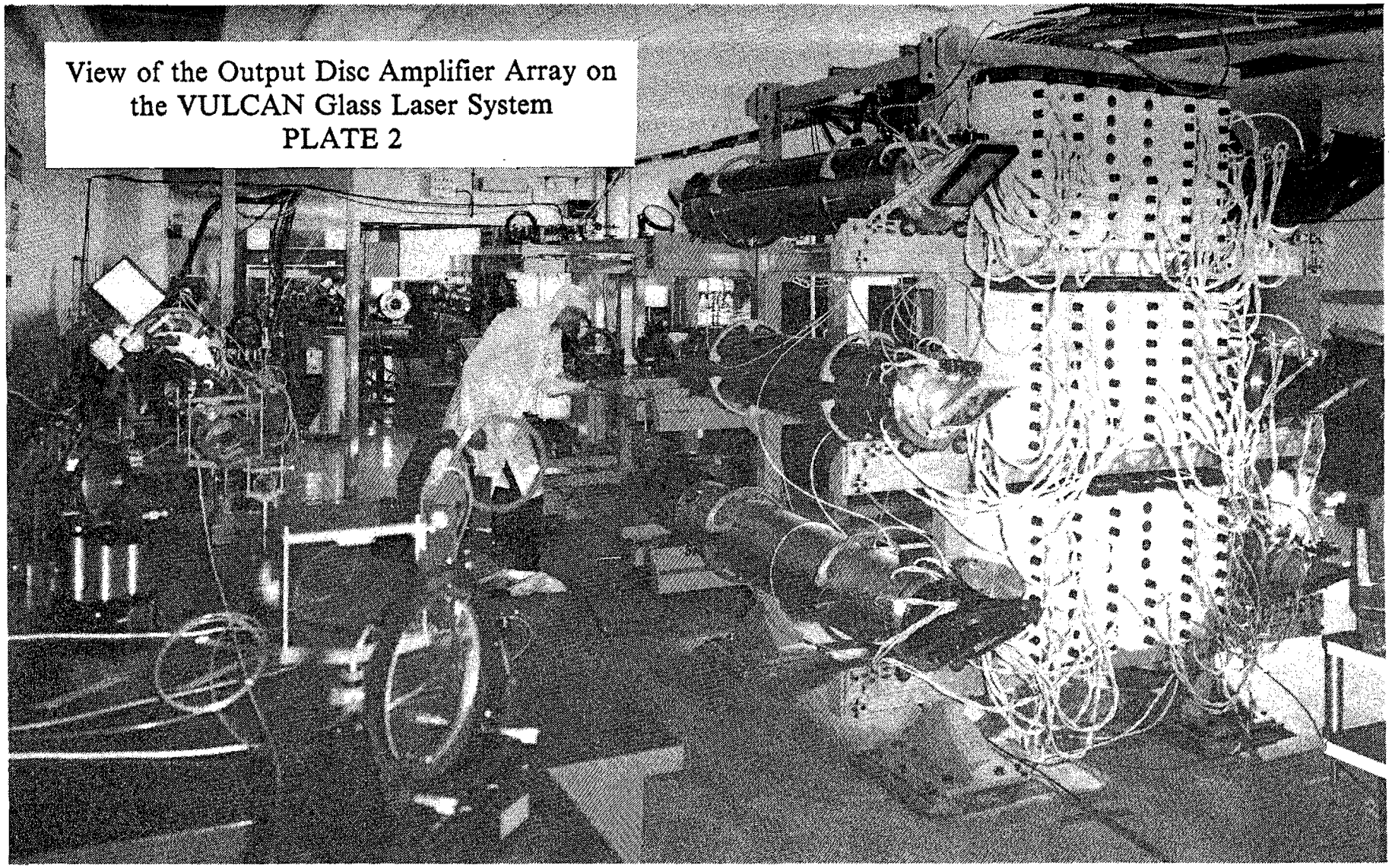

View of the Output Disc Amplifier Array on the VULCAN Glass Laser System
PLATE 2

need an order of magnitude increase in accelerating gradient to produce a collider of reasonable length.

There are several novel acceleration techniques under investigation, for example the Laser-plasma accelerator (beat-wave), the wake-field accelerator and the plasma-wake-field accelerator.

The Beat-wave concept was proposed by Tajima and Dawson in 1979 (2.1). The transverse electro-magnetic field of a laser is ineffective for acceleration, and the beat-wave concept couples the transverse field to a longitudinal wave. It is possible to generate extremely high accelerating gradients as the plasma is not susceptible to break-down since it is already ionised.

Figure 1 shows how the Beat-wave process occurs. Two intense laser beams of slightly different frequencies (ω_1, ω_2) are injected into a plasma whose difference frequency ($\omega_{diff} = \omega_1 - \omega_2$) is resonant with the natural plasma frequency, (ω_p), of the plasma. At resonance the electrons bunch to produce a longitudinal wave. Injection of electrons into this wave can produce acceleration.

If the plasma bunches completely then the longitudinal accelerating field, eE, is given by (2.4)

$$eE = mc\omega_p = mc^2(4\pi nr)^{1/2}/137 \qquad 2.1$$

where e, m and r are the charge, mass and classical radius of the electron respectively, and n is the plasma density. In a typical plasma it is possible to obtain densities of 10^{17} per cm^3 which would produce an accelerating gradient of 20 GeV per meter.

In a single stage device the electrons would get out of phase with the accelerating wave, therefore in a real accelerator several stages of amplification would be necessary. To avoid adverse effects from movement of the ions in the plasma it is necessary to use short laser pulses (50 - 100 ps).

The energy gain to the accelerated beam is proportional to γ the relativistic factor associated with the plasma phase velocity, v_{ph} where

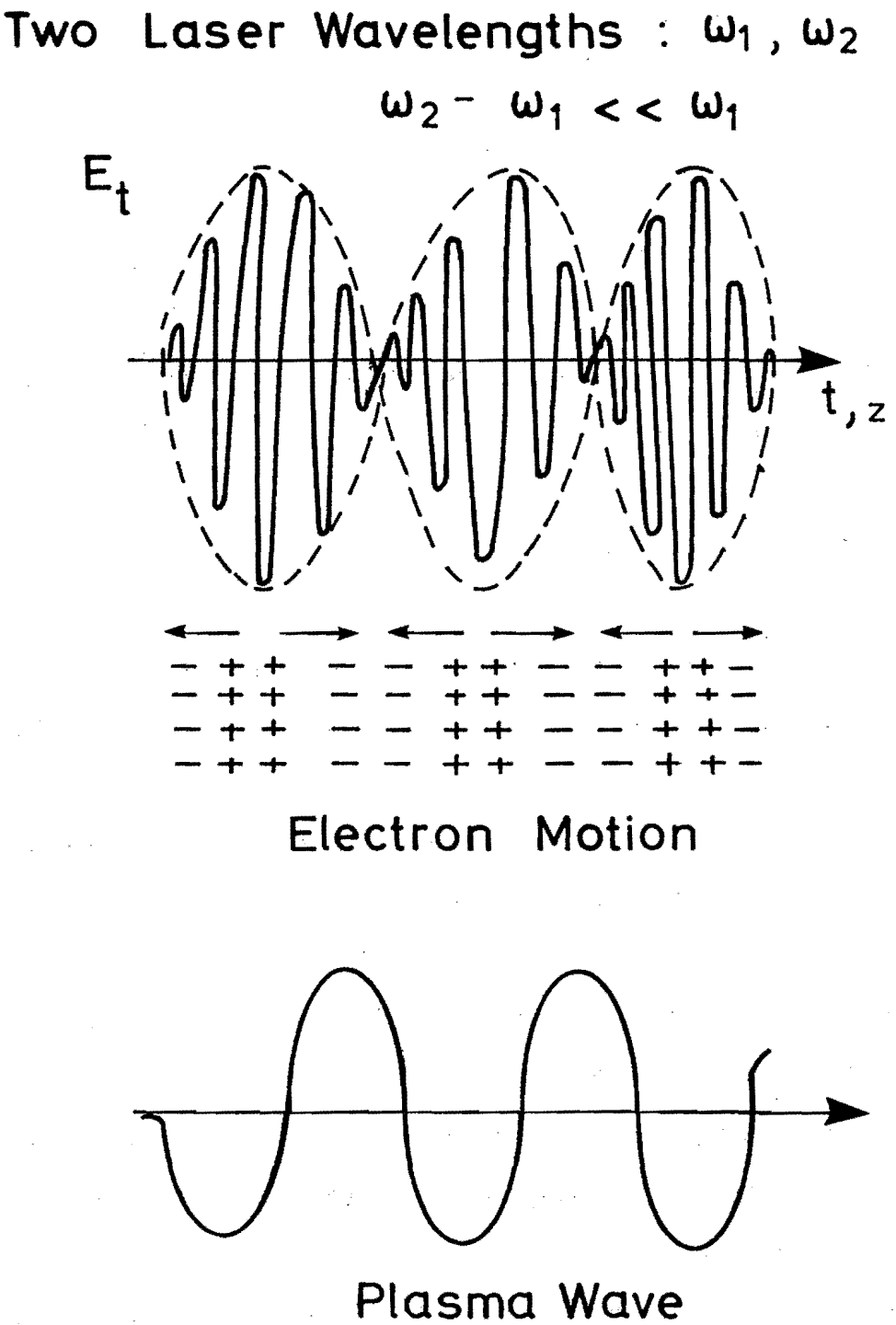

THE BEAT-WAVE PROCESS
FIGURE 1

$$\gamma = [1 - (v_{ph}/c)^2]^{-1/2} \qquad 2.2$$

where v_{ph} is given by

$$v_{ph} = c[1 - (\omega_p/\omega)^2]^{1/2} \qquad 2.3$$

from 2.2 and 2.3 the energy gain is therefore proportional to

$$\gamma^2 = (\omega/\omega_p)^2 \qquad 2.4$$

With the experiments at RAL, using 1 micron radiation, the relativistic factor associated with the wave is about 100.

2.4 The RAL Beat-Wave Experiment.

A series of experiments have been conducted in the USA, Canada and the UK to study the generation of Beat-waves. The experiments in the USA and Canada (2.2 and 2.3) used Carbon Dioxide lasers, operating at 9.6 and 10.6 microns. The relativistic factor associated with these wavelengths is about 10, therefore experiments at RAL, with a relativistic factor of 100 produce fields which are more relevant to an accelerator.

There were two main experimental goals for the RAL experimental program:-

(i) To demonstrate through photo-ionisation the production of a uniform density plasma. These experiments required a single ionising beam, therefore did not require extensive facility modifications, allowing them to be conducted in parallel with other scheduled experiments.

(ii) To demonstrate the existence of a relativistic Beat-wave. For these experiments the system modifications described in Chapters 3 and 4 were necessary. These extensive system modifications meant that these experiments had to be scheduled alone.

CHAPTER 3

OSCILLATOR DEVELOPMENT

Abstract

This chapter describes the development of a pulse generation system to provide pulses for the Beat-wave experiment. The first oscillator system described used two amplifying media housed in the same cavity to generate the two pulses. It was necessary to change the initial design due to problems with stability, and a second system is described in which the two pulses were generated in separate cavities.

3.1 Introduction

Experimental Requirements

The oscillator systems developed for the Beat-wave experiment generated pulses suitable for injection in the VULCAN glass laser amplifier chains. The requirements for these pulses were:

(i) Two wavelength operation.

(ii) Short pulsewidths of about 150 - 300 ps in duration.

(iii) Single pulse energies of approximately 100 - 500 micro Joules.

(iv) Synchronisation of the two pulses to better than 30 ps.

(v) Good shot to shot reproducibility.

These requirements are discussed below.

Two Wavelength Generation

The two wavelengths were generated from a Nd:YLF crystal operating on the 1.053

micron line and a Nd:YAG crystal operating on the 1.064 micron line. Nd:YLF is a uniaxial crystal which has two lasing lines, 1.047 microns and 1.053 microns. Selection between the two lines is achieved by changing the crystal orientation relative to the polarisation of the light within the cavity. The 1.047 micron line has the lower threshold for lasing but can be discriminated against by inserting a suitably orientated polariser into the cavity. The 1.064 micron line is the lowest threshold lasing wavelength in Nd:YAG, discrimination against the other frequencies is achieved by operating the oscillator just above the lasing threshold for this line. As described in Chapter 1 these two wavelengths are both widely used on high power laser systems as they are a good match to the peak gains produced from silicate and phosphate glass amplifiers.

Basic Oscillator Design

The oscillators used to generate the beat-wave pulses were based on the design of Kuizenga and Siegman (3.1) for use at the Lawrence Livermore National Laboratory in high power laser systems. The oscillators are actively mode-locked and actively Q-switched, operated in such a way as to enable their outputs to be synchronised with other pulses and external events. A further advantage of this design is a high shot to shot reproducibility. This is due to the ability to control the cavity flux prior to Q-switching by generating a stable prelase, achieved by the use of a high stability power supply for flashlamp pumping. This type of oscillator is now used on several neodymium high powered laser systems. This proven design has been used for this application but modified in such a way to generate the two pulses required.

The oscillator design is that of a stable resonator, consisting of a high reflecting 5 meter focal length rear mirror and an optically flat partially transmitting front mirror as shown in figure 2. The degree of transmission is optimised for the gain of the active medium and provides the pulse output. The gain cross section of the

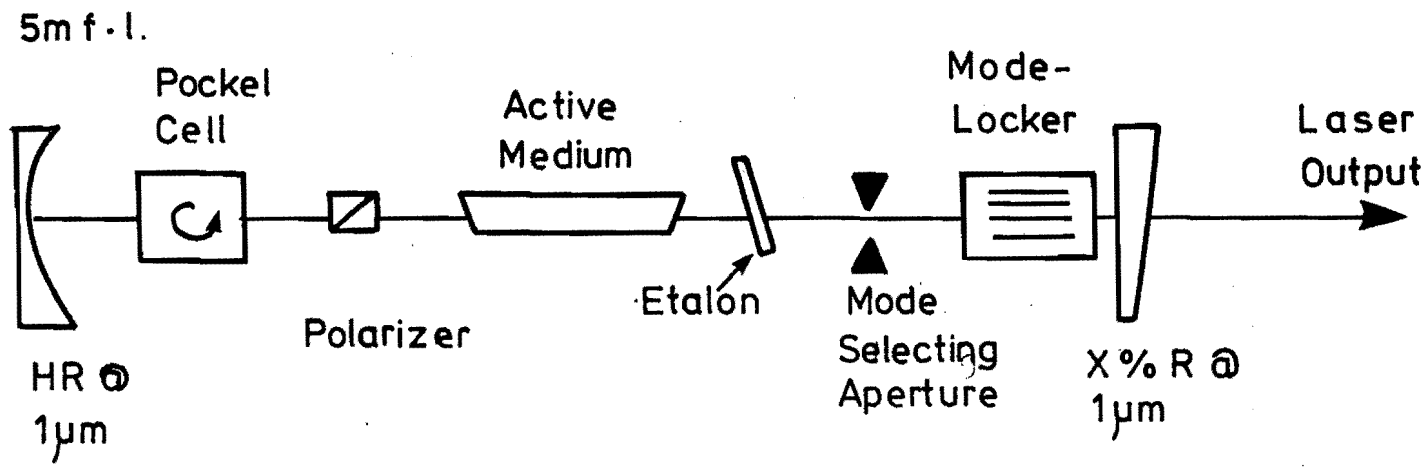

THE BASIC OSCILLATOR CONFIGURATION
FIGURE 2

active medium determines the operating wavelength, with additional wavelength selectivity provided by a series of prisms or a polariser. A Pockels cell is used to Q-switch the cavity and an acousto-optic modulator to mode-lock the pulse. The bandwidth is controlled by placing an etalon within the cavity giving control of the pulse duration.

A single flashlamp in the oscillator head is used to pump the laser rod. The flashlamp is driven by a current stabilised high voltage power supply allowing time for the mode-locking process to reach completion. The sequence of events leading to pulse generation is described in figure 3. Synchronous with the switching of power to the flashlamp, an r.f. voltage is applied to the mode-locker and an intra cavity dc loss is introduced by applying a voltage to the Pockels cell. The cavity reaches threshold and the laser goes through relaxation oscillations which eventually die out to produce a quasi cw output prelasing level. At this stage the mode-locking process has reached completion, and the Q-switch loss is now reduced, generating a giant Q-switched pulse which produces a train of mode-locked pulses at the output separated in time by the cavity round trip.

3.2 Theory

3.2.a Q-switch Build-up Time

The flux within the cavity grows according to (1.13)

$$\Phi = \Phi_i \exp (2\alpha l - \gamma)\, t/T_R \qquad 3.1$$

where: T_R is the round trip time of the cavity, Φ_i is the initial flux at the time of Q-switching, α is the gain coefficient, l is the cavity length and γ is the total of the round trip losses in the cavity. This equation assumes that the inversion in the cavity remains unchanged, which is a valid approximation until the flux in the cavity

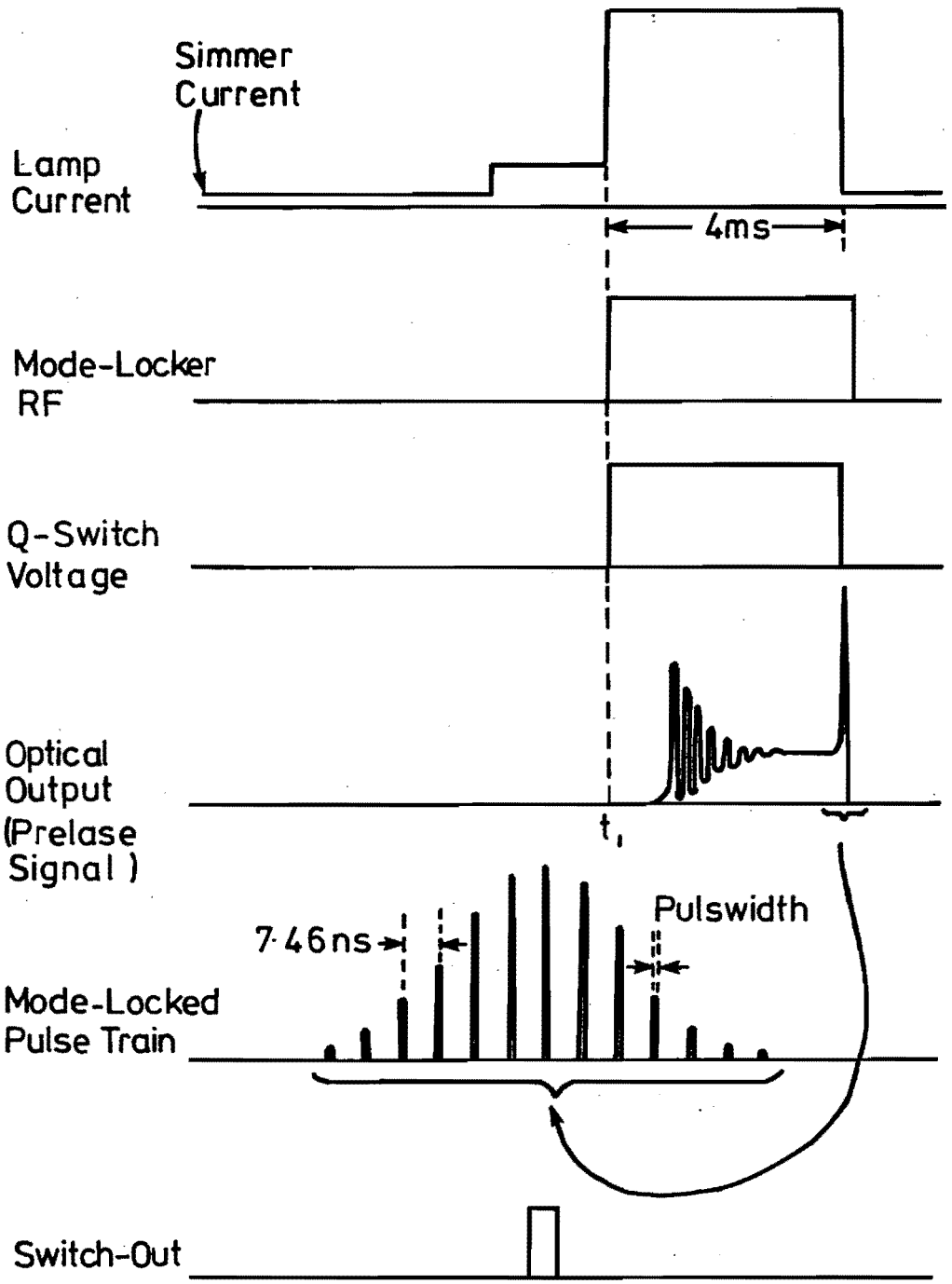

OSCILLATOR SEQUENCE OF EVENTS
FIGURE 3

becomes a significant fraction of the peak radiation density.

The build up time from the voltage being removed from the Pockels cell to the generation of the Q-switch pulse up to 0.1 Φ_m, the maximum flux within the cavity, is given by (1.13)

$$T_{Q\text{-switch}} = \frac{T_R \ln (0.1\, \Phi_m/\Phi_i)}{2\alpha l - \gamma} \qquad 3.2$$

From equation 3.2 the Q-switch build-up time is dependent on the initial flux within the cavity. If the other parameters within the equation are kept constant and the initial flux is consistent from shot to shot then the Q-switch build-up time will also be consistent. For a cavity of the type described above the prelase level sets the initial flux, therefore if the prelase level is stable the Q-switch build-up time will be extremely reproducible. This reproducibility makes possible the synchronisation of the mode-locked pulses to external events.

3.2.b Pulsewidth Dependence on Cavity Parameters

The theory of the generation of pulses with the oscillator design described above has been rigorously analysed by Kuizenga and Siegman (3.1). The model used follows the development of a pulse as it circulates the cavity. The important components considered in the theory include the mode-locker which imposes a time dependent loss to the circulating pulse and the Q-switch which can be treated as a d.c. loss during the pulse forming period. Also included is the amplitude gain bandwidth of the active medium, and frequency dependent etalon transmission. From this theory the steady state pulse-widths generated from such cavities are given by

$$t_p = \frac{(2\ln 2)^{1/2}}{\pi} \cdot \frac{1}{\theta_m^{1/2}} \cdot \frac{1}{f_m^{1/2}} \cdot \left(\frac{g}{\Delta f^2} + \frac{1}{\Delta f_e^2} \right)^{1/4} \qquad 3.3$$

where; θ_m is the depth of modulation, f_m is the frequency of modulation, g is the saturated gain at line centre, Δf is the line-width and Δf_e is the effective bandwidth of an etalon, given by

$$\Delta f_e = 2c \{ \pi h (n^2-1) \}^{-1} \qquad 3.4$$

where; h is the etalon thickness and n is its refractive index.

It can be seen from equation 3.3 that the pulsewidth generated is dependent on the gain and the bandwidth of the active medium, and the frequency and efficiency of the mode-locker. If an etalon is present this also has to be considered. There are only three parameters that can readily be changed experimentally; the round trip gain of the cavity, the modulation depth of the mode-locker and the thickness of the etalon.

To produce a consistent prelase, a cavity of this type is operated at a constant level above threshold. To generate this prelase level the round trip gain in the cavity has to be altered, accomplished by changing the losses in the cavity or the gain of the active medium. Variation in the losses is achieved by either changing the Q-switching loss or by changing the reflectivity of the front mirror.

Applying equation 3.3 it was possible to determine the necessary operating conditions for the oscillators to generate the required pulsewidths. It was also important before building the oscillators to have an understanding of how sensitive the pulsewidths generated in the Nd:YAG and Nd:YLF were to alterations in the different cavity parameters.

Pulsewidth Dependence on Gain

Calculations were made using equation 3.3 in order to investigate the variation of pulsewidth with gain. The graph in figure 4 shows the results of these calculations. Two different cases were considered; one with no etalon in the cavity and in the other a 3 mm etalon inserted into the cavity. In both cases the bandwidth used was

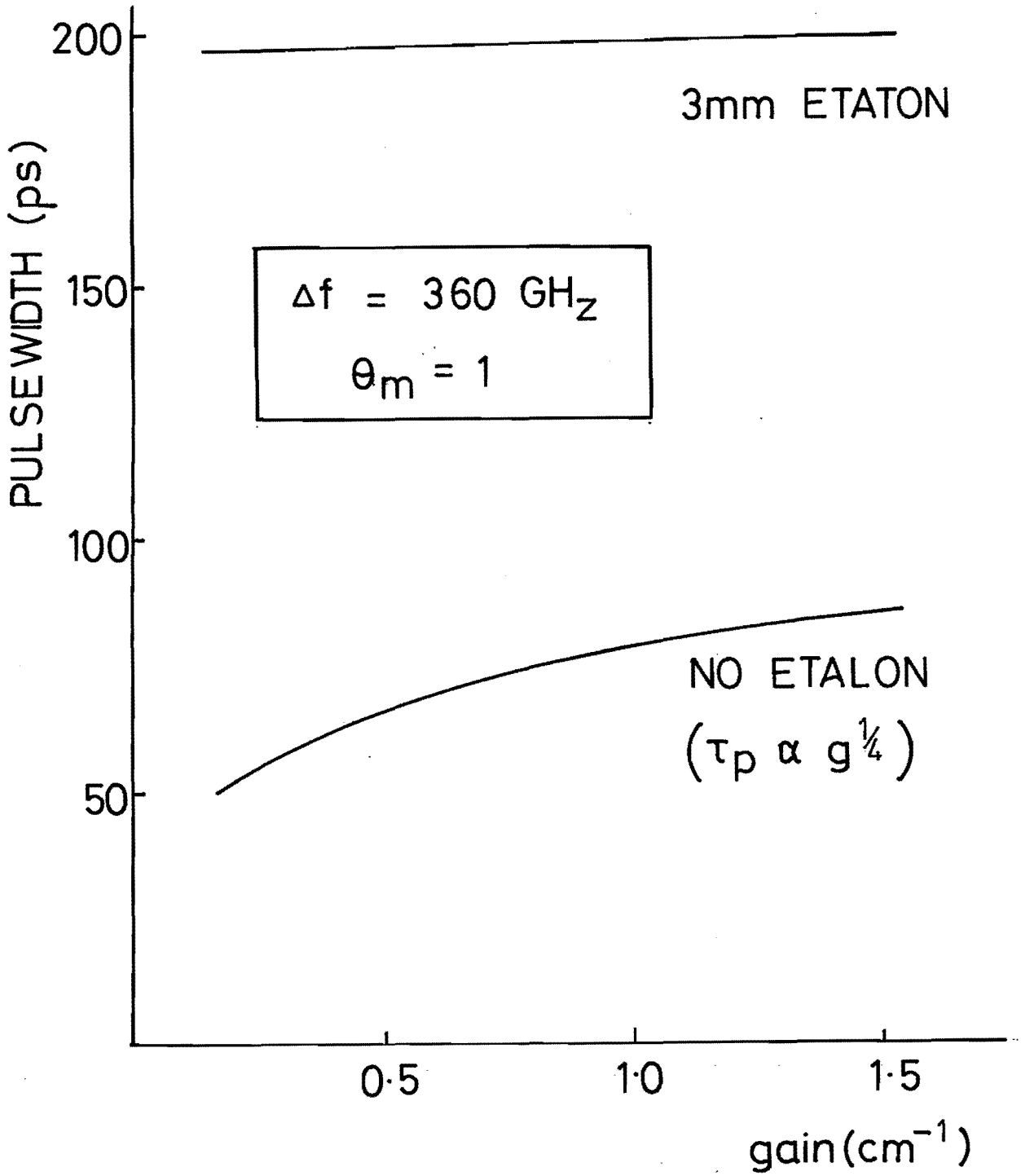

PULSEWIDTH DEPENDENCE ON GAIN
FIGURE 4

that of Nd:YLF of 360 GHz, the modulation frequency was 67 MHz and the depth of modulation was kept constant at a value of 1.0.

With no etalon in the cavity a small change in pulsewidth is observed as the gain is changed. This change is expected as, from equation 3.3, the pulsewidth is proportional to the fourth root of the gain. This does not lead to any significant change in pulsewidth over the experimental operating range. With the 3 mm etalon inserted into the cavity the bandwidth of the etalon dominates the pulse forming process over the gain bandwidth of the medium. This produces only a one percent change in the pulsewidth as the gain is varied from 0.2 to 1.5 per cm. This is significantly greater than the variation of gain possible in the experiment. The experimental limitations are set by the amount of energy that needs to be extracted and the pumping limitations of the power supply to the flashlamp. Therefore it is not practicable to tune the pulsewidth by adjusting the gain of the cavity.

Pulsewidth Dependence on Etalon Thickness

Equation 3.3 was applied to investigate the variation of pulsewidth as the etalon thickness was changed. The relationship was calculated for both Nd:YAG and Nd:YLF, using bandwidths of 180 GHz and 360 GHz respectively (from Table 1), the gain of the cavity was set to 0.43 per cm and the modulation depth to 1.0. The gain used was a value calculated for a Nd:YAG cavity configuration and due to the very low dependence of the gain on the pulsewidth this value was used throughout. The results are presented in figure 5.

With no etalon in the cavity there is a 30% difference in pulsewidth between the two laser hosts. This difference has since been verified experimentally and the two points are shown in figure 5. In equation 3.3 the bandwidth contribution to the pulsewidth consists of two components a gain bandwidth term and an effective etalon bandwidth term. With no etalon the effective etalon bandwidth is infinite eliminating that term from the equation, therefore the pulsewidths from the two

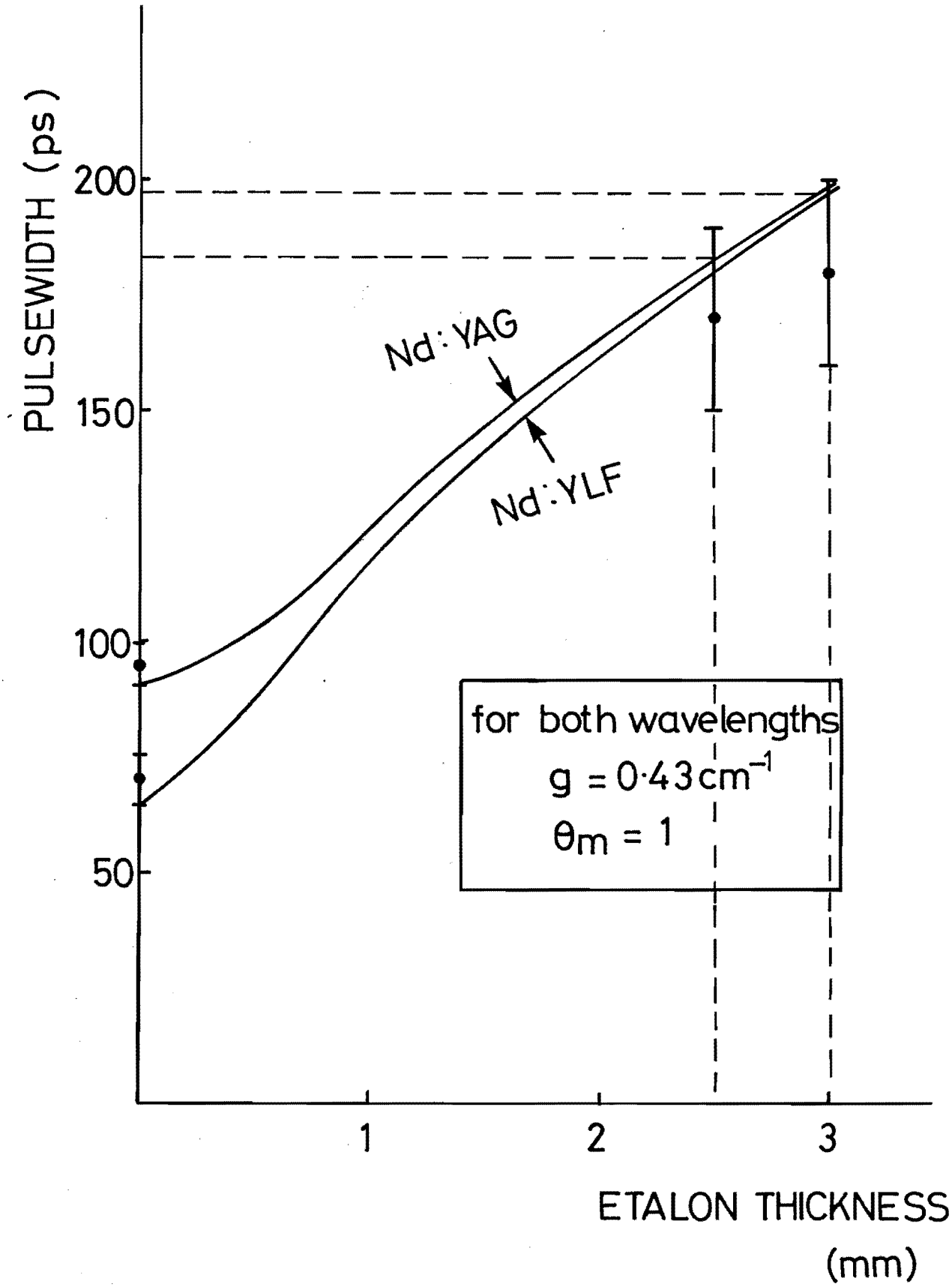

PULSEWIDTH DEPENDENCE ON
ETALON THICKNESS
FIGURE 5

cavities are dictated by the difference in gain bandwidths. As the etalon thickness is increased the bandwidth of the etalon begins to dominate. With a 3 mm etalon in the cavity there is only a 1% difference in pulsewidth and with an 11 mm etalon the difference is down to 0.26 %. Superimposed on the theoretical curves in figure 5 are some experimental points using a 2.5 mm etalon with Nd:YAG and a 3 mm etalon with Nd:YLF showing reasonable agreement between theory and experiment. Some measurements have also been taken using a 10 mm etalon with Nd:YLF. The agreement between experiment and theory was not as good producing an experimental value of 300 ± 30 ps and a theoretical value of 377 ps. These calculations have shown that by using suitable etalons it is practicable to produce the required pulsewidth.

Pulsewidth Dependence on Modulation Depth

The variation of pulsewidth as the modulation depth of the mode-locker was then investigated using equation 3.3. The calculations were using Nd:YAG with a bandwidth of 180 GHz and a peak gain of 0.43 per cm. The results of this analysis are shown in figure 6. It can be seen that a reduction in modulation depth results in an increase in the pulsewidth. By using a limited number of etalons, and fine tuning the modulation depth, it is possible to cover the entire range of pulsewidths from 100 ps to 1 ns.

These theoretical results made it possible to design the oscillator configuration, for example by selection of the appropriate etalons, to produce the required pulse durations for the Beat-wave experiment.

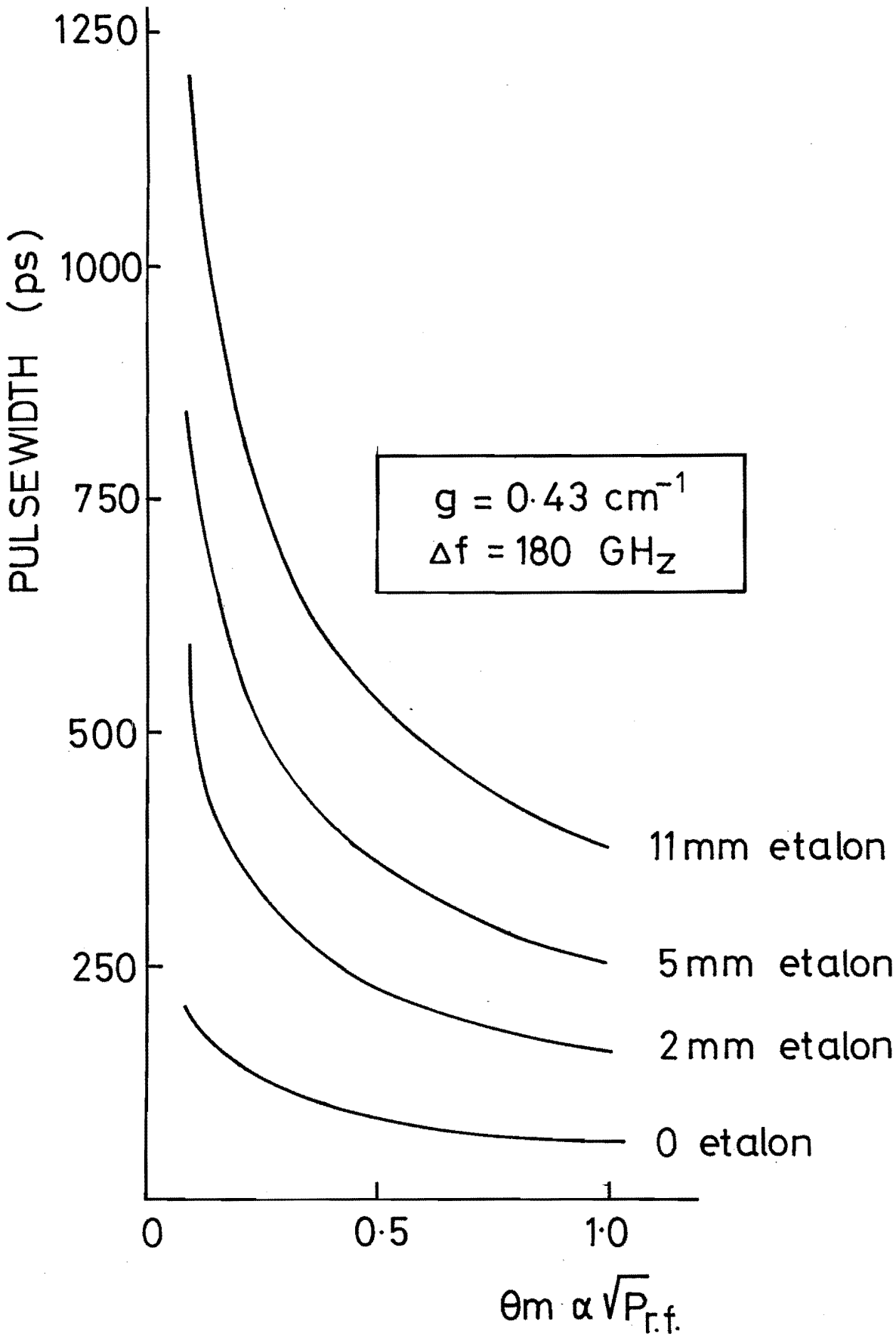

PULSEWIDTH DEPENDENCE ON
MODULATION DEPTH
FIGURE 6

3.3 OSCILLATOR DESIGN

3.3.a Single Cavity - HYDRA

To generate the two wavelengths the oscillator was designed with both lasing media housed in the same cavity. Q-switching and mode-locking components common to both lasing lines should ensure synchronous generation of the two pulses. This assumed that the cavity round trip dispersion was small enough to allow the cavity length to be matched to the mode-locking r.f. for both wavelengths. Initial calculations indicated that this would be the case although accurate refractive indices were not available for all the components within the cavity. The Q-switch build-up time is given by equation 3.2. The ($2\alpha l - \gamma$) term should be the same in the two cases as the gains of the media were set to produce a lasing level just above threshold in both cases eliminating any loss differences between the two wavelengths. The initial flux level in both cases was set by the prelase level which were nominally the same therefore the Q-switch build-up times of the two wavelengths should be the same.

Oscillator Configuration

Schematics of the oscillator configurations used are shown in Figure 7. The configurations are basically similar, each consisting of a Nd:YAG rod to lase at 1.064 microns and a Nd:YLF rod, suitably orientated with respect to the polariser, to lase at 1.053 microns. The rest of the components in the cavity are the same as described in the introduction to this chapter consisting of a stable resonator housing an electro-optic Q-switch, an acousto-optic mode-locker, and a transverse mode selecting aperture.

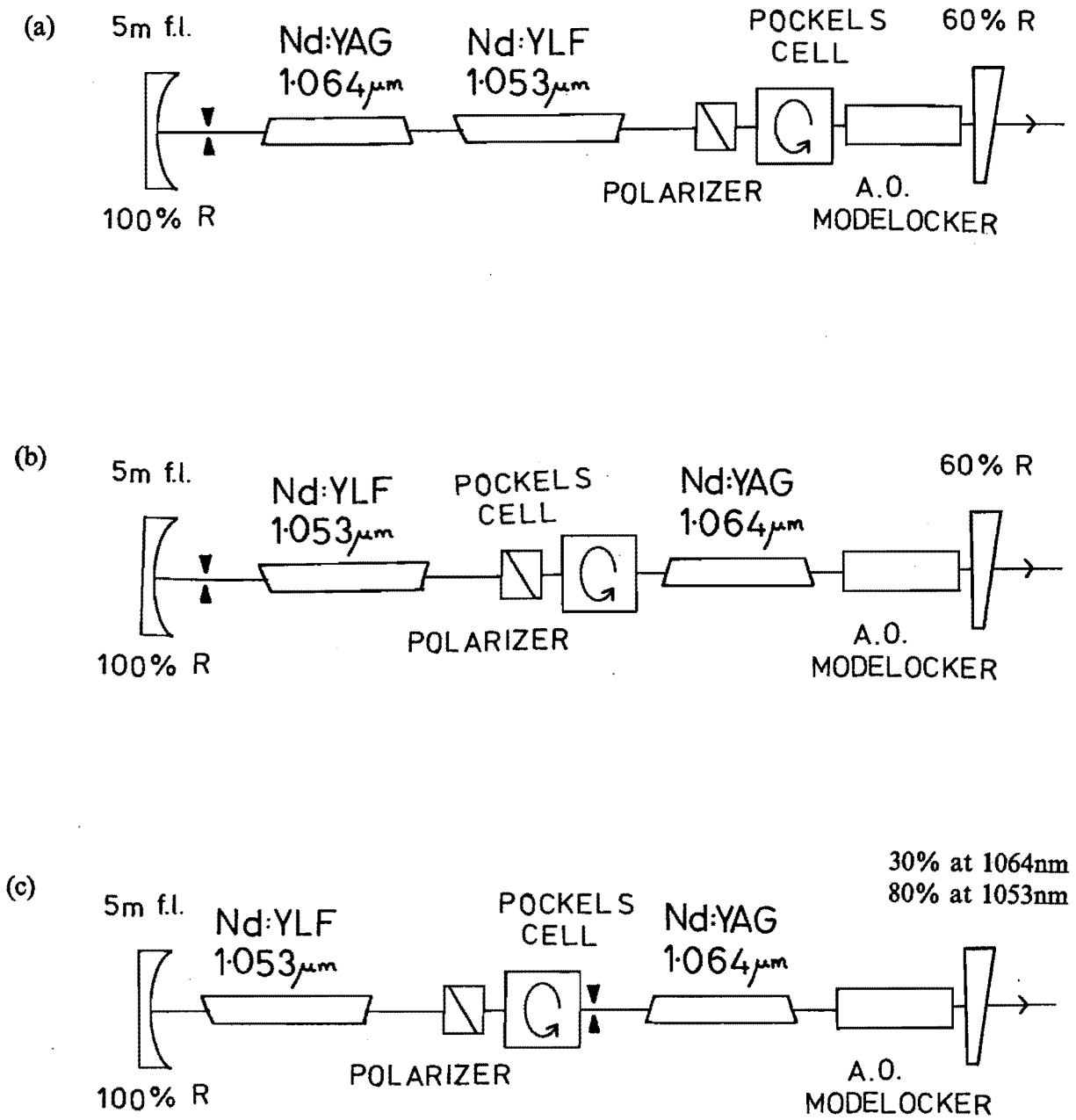

HYDRA BEAT-WAVE OSCILLATOR CONFIGURATIONS

FIGURE 7

Cavity Alignment

To align the components within the cavity a HeNe laser beam was injected through the back of the rear mirror. The HeNe was then aligned along the cavity axis. The beam path was then defined by inserting the mode selecting aperture into the cavity and using a far field reference point, usually a cross on the laboratory wall. The oscillator components were then centred on this beam. The two resonator mirrors were initially aligned using the reflected HeNe beams. One of the laser power supplies was then fired at a high repetition rate whilst adjusting the output mirror until laser output was achieved. Mirror alignment was then optimised to maximise the lasing signal, which was incident onto a photodiode coupled to an oscilloscope. The Pockels cell was aligned by centring the Maltese cross pattern generated when observing the diffused HeNe passing through the cell between crossed polarisers.

Mode-locker Alignment

To align the mode-locker it was necessary to ensure that the transducer on the crystal was resonant with the applied rf. voltage. The resonance is dependent on the mode-locker temperature which is controlled using a thermally stabilised coolant supply. The modulator is operated above the ambient temperature to prevent condensation on the crystal surfaces, giving a tuning range of 23 - 35 degrees C. A Bird r.f. reflectometer was then placed in the r.f. line to the mode-locker. As the r.f. frequency was scanned a number of minima and maxima in reflected power were observed. A scan of one of these minima is shown in Figure 8. The exact minima chosen is dictated by a convenient cavity length, long enough to house the components and short enough to be of practical length for the optical bench. For these oscillators the nearest minima above 67 MHz is used which corresponds to a round trip time of about 7.5 ns. As can be seen from the figure the reflected power minima does not read zero. This is probably due to imperfections in the bonding of

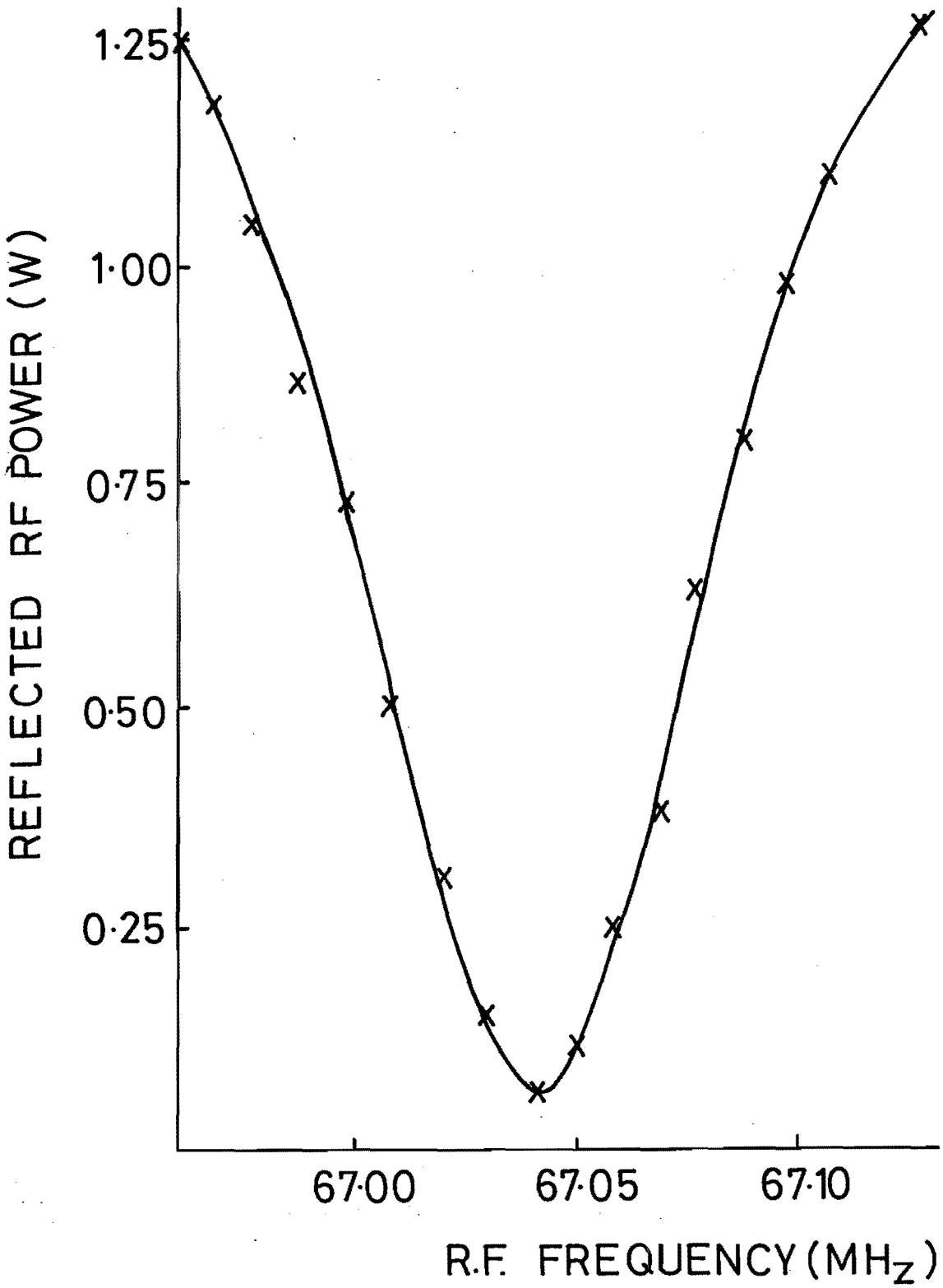

RESONANT RF VOLTAGE TUNING
OF THE MODE-LOCKING CRYSTAL
FIGURE 8

the transducer to the quartz crystal. The r.f. frequency was then set at this minima value to provide maximum coupling.

To obtain the maximum diffraction efficiency of the light wave by the acoustic wave within the mode-locker it was necessary to orientate the crystal such that the acoustic wave was at the Bragg angle with respect to the cavity axis. The Bragg angle is defined by (3.2)

$$\theta_{Bragg} = \lambda f/2V \qquad 3.5$$

where; λ is the optical wavelength (1.053 microns), f is the acoustic frequency (67 MHz) and V is the acoustic velocity in quartz (0.006 meters per second). Using these values the Bragg angle was calculated to be 6 milli-Radians.

To align the crystal at the Bragg angle a cavity was established by inserting a mirror between the mode-locker and the other cavity components (figure 7). The mirror was plane parallel such that the exit beam from this cavity propagated through the mode-locker on exactly the same path as for the normal cavity. With the normal front mirror detuned the intra-cavity mirror was aligned to lase without moving the cavity rear mirror. The output beam was then incident onto a photo-diode coupled to a Gould digital storage oscilloscope. As the angle of the modulator was then scanned a series of maxima and minima signals were observed on the detector. The two deepest minima either side of a central maximum correspond to the Bragg angles.

The crystal orientation was then set to one of these two minima. It was then necessary to match the cavity length to the modulator frequency to ensure efficient mode-locking and stable pulse generation. The intracavity mirror was first removed and the front mirror realigned for efficient lasing. By observing the prelasing diode signal the cavity length was then scanned to find the maximum signal height corresponding to the correct cavity length. The diode response is shown in Figure 9. An obvious feature is the very sharp maximum observed at the correct cavity length. Using this method it is possible to adjust the cavity length to within 10 microns of

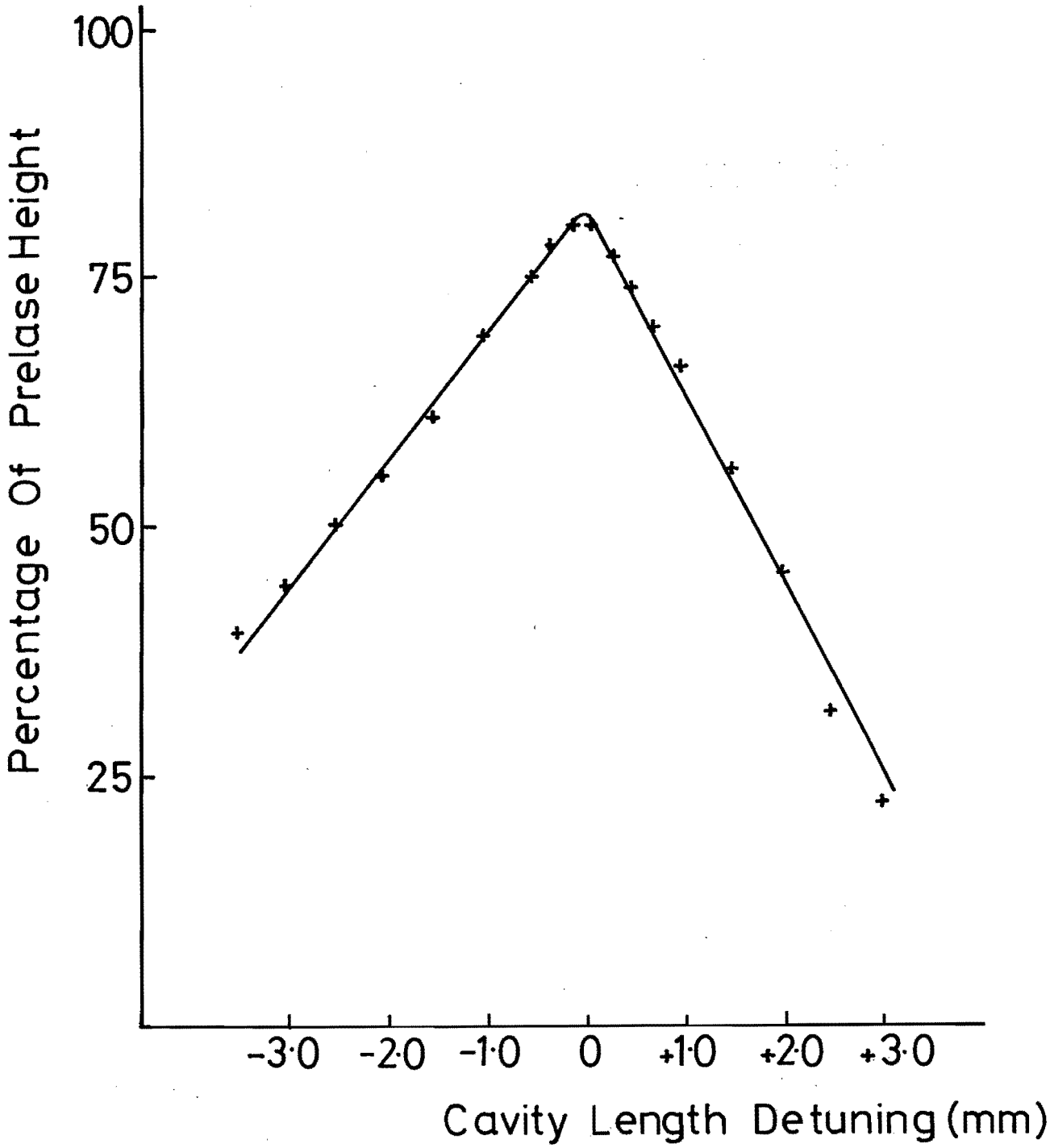

MATCHING THE CAVITY LENGTH TO
THE MODE-LOCKING FREQUENCY
FIGURE 9

the correct length.

Cavity Operation

The initial design of oscillator is shown in figure 7 configuration (a). Each of the oscillator heads were operated independently in order to set up the cavity and the individual prelases. It was found that the optimum cavity lengths for the two wavelengths were within five microns of each other, which should enable stable operation at the two wavelengths for a single cavity length.

The two independent prelase signals generated are shown in Plate 3. It can be seen that relaxation oscillations were formed which die out after about 1 ms to form a quasi-cw level. This level was found to be very stable and could be sustained for several milliseconds. This was only true if the cavity length was correct to about 5 microns, which could be adjusted whilst observing the prelase. A source of instability was feedback of the output pulse into the cavity from spurious reflections. This caused gain depletion during the prelase period causing the stable prelase to once again break into relaxation oscillations. It was therefore necessary to ensure that detector windows, polarisers etc were not exactly perpendicular to the beam.

Under normal operating conditions both laser heads were run together. The prelase signal generated under these conditions is shown in Plate 4. Although the prelase shown is stable it proved difficult to achieve. It was found that allowing the relaxation oscillations of one wavelength to die out before the oscillations of the other began produced a much more stable prelase than allowing them both to build together, hence in plate 4 two sets of relaxation oscillations are observed.

It was possible to monitor the relaxation oscillations in more detail by increasing the sweep rate on the oscilloscope. The frequency of the oscillations was found to be different for the two different wavelengths. The frequency of the relaxation oscillations is given by (3.3)

HYDRA PRELASE OUTPUTS

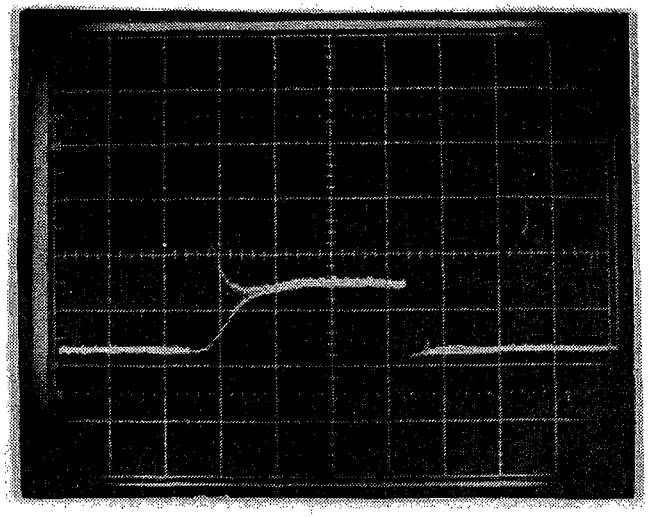

1 ms / div

Nd:YLF 1053 nm

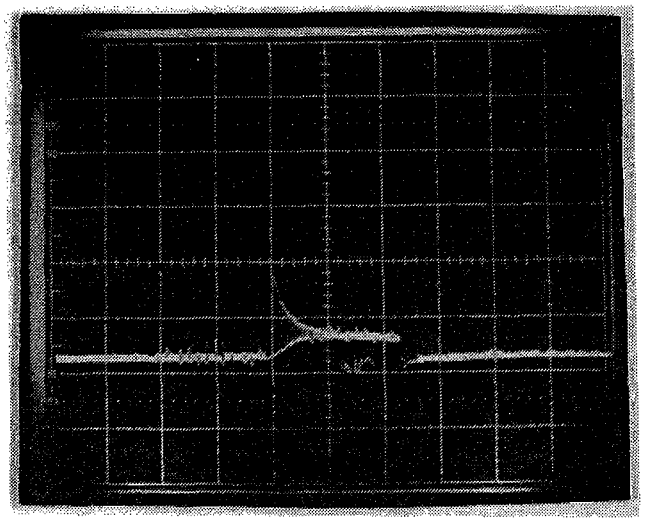

1 ms / div

Nd:YAG 1064 nm

SINGLE WAVELENGTH OPERATION

PLATE 3

HYDRA PRELASE

OUTPUT

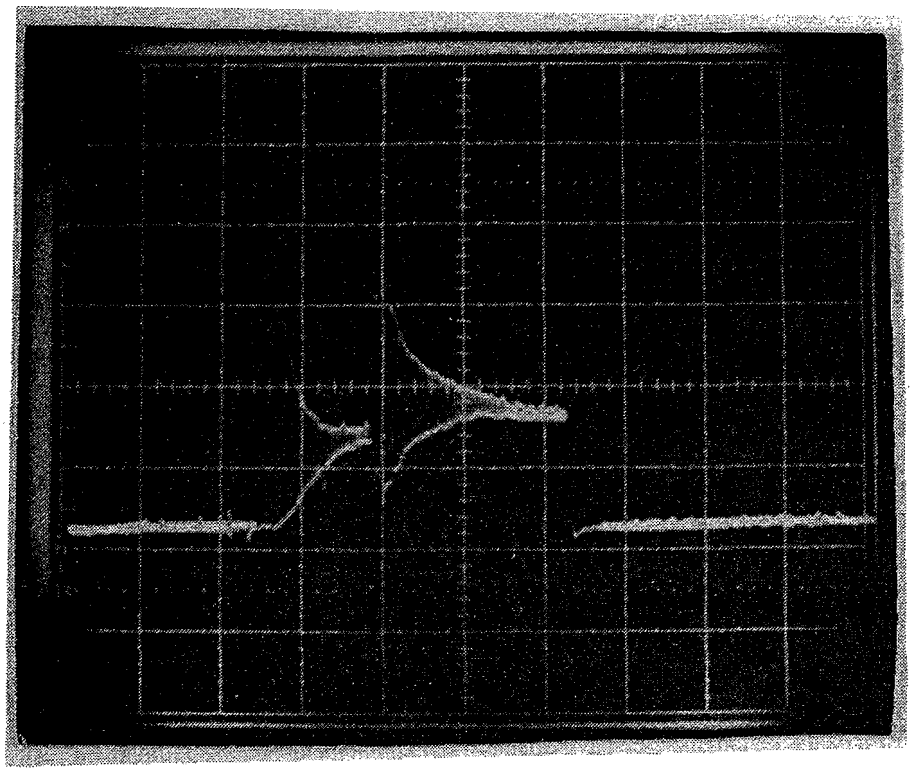

1 ms / div

TWO WAVELENGTH OPERATION

PLATE 4

$$\omega_{rel} = (\sigma I / t_c h\nu)^{-1/2} \qquad 3.6$$

where; σ is the stimulated emission cross section, t_c is the decay time constant of the laser radiation and I is the intensity of the radiation in the cavity. From this equation the lower the circulating power density, I, and hence the output from the cavity, the higher the relaxation oscillation frequency. Since the output intensity from the two cavities was significantly different, the relaxation oscillation frequency would therefore also be different.

Interaction Between the Lasing Media

Using the cavity configuration, described above, it proved difficult to achieve stable prelasing. It was observed that if the pumping to the Nd:YLF head was turned down below the threshold for lasing the 1.064 micron prelase output was found to be stable, but under the same conditions if the pumping to the Nd:YAG head was turned down below threshold instabilities were still evident on the 1.053 micron prelase output. It was believed that there was some interaction between the two active media on the 1.053 micron line. A list (3.4) of all the possible room temperature transitions in Nd:YAG shows a reasonably strong transition at 1.052 microns, which was possibly being pumped by the 1.053 micron output.

Provision of Isolation Between Lasing Heads

It was decided to provide some form of isolation between the two amplifying media. This was achieved by placing the Q-switching Pockels cell and polariser between the two rods as shown in Figure 7 cavity (b). This would greatly reduce the amount of light seen by either head produced by the other during the prelasing period. When this cavity was operated stability did seem to improve although not conclusively. With intricate adjustment of the relative heights of the prelases and by altering the

relative delays to the start of the pelasing it was possible to obtain prelase stability on about 80% of the shots.

Cavity Q-switching

When the cavity was Q-switched a train of high energy pulses was generated. A typical pulse train output is shown in Plate 5. The number of pulses contained within the pulse train could be altered by changing the voltage applied to the Pockels cell. As the voltage was reduced the number of pulses increased although the energy contained within any single pulse reduced. This is shown graphically in figure 10. A voltage was chosen such that there was sufficient energy in a single pulse but not enough energy to cause damage to components within the cavity.

To measure the relative amplitudes of the two wavelengths it was possible to turn the laser heads off alternately and monitor a single wavelength. When the prelase became unstable the relative Q-switch build up times would jitter from shot to shot. This was because as the Q-switching process began the initial optical fluences were not the same for the two wavelengths. Such a situation is shown in Plate 6. The instability in this case was induced by turning down the lamp current to the Nd:YAG laser head. This eliminated the stable prelase of the 1.064 micron wavelength producing random Q-switch build-up times between the two wavelengths. The Q-switched envelope can be seen to consist of about 60% 1.053 micron and 40% 1.064 micron output.

A streak camera was then set up to look at the output pulses from the cavity. A densitometer trace of a streak-camera output is shown in Figure 11. The pulsewidths generated by the cavity were measured when both wavelengths or a single wavelength were present. The pulsewidth did not appear to change in either case, indicating good synchronisation between the two wavelengths. Although two pulses of significantly different amplitudes were difficult to analyse.

HYDRA Q-SWITCH

ENVELOPE

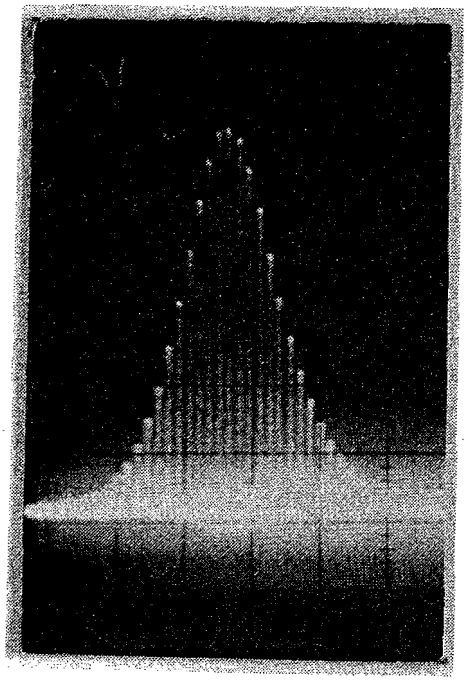

Pulse Seperation = 7.5 ns

1053 nm + 1064 nm
SYNCHRONOUS OPERATION

PLATE 5

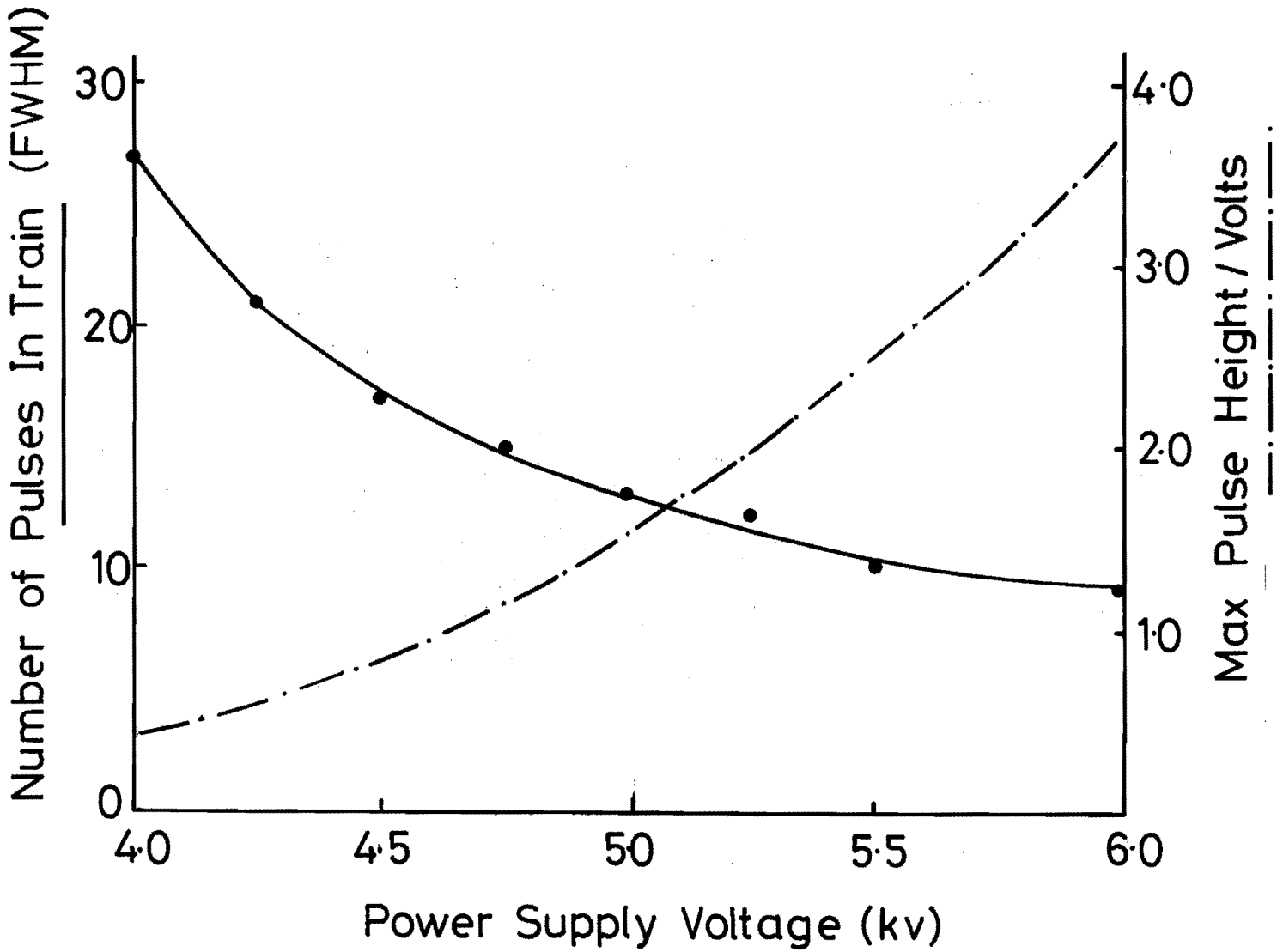

Q-SWITCH VOLTAGE EFFECTS ON THE
LASER PULSE ENVELOPE
FIGURE 10

HYDRA PULSE TRAIN OUTPUT WITH INDUCED INSTABILITY

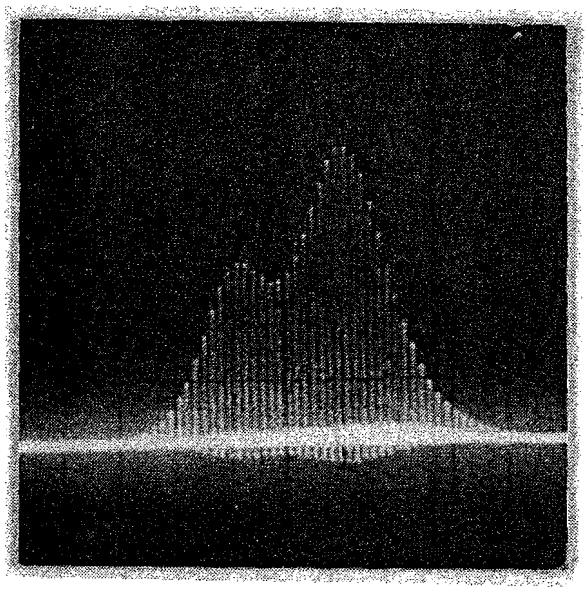

Pulse Separation = 7.5 ns

PLATE 6

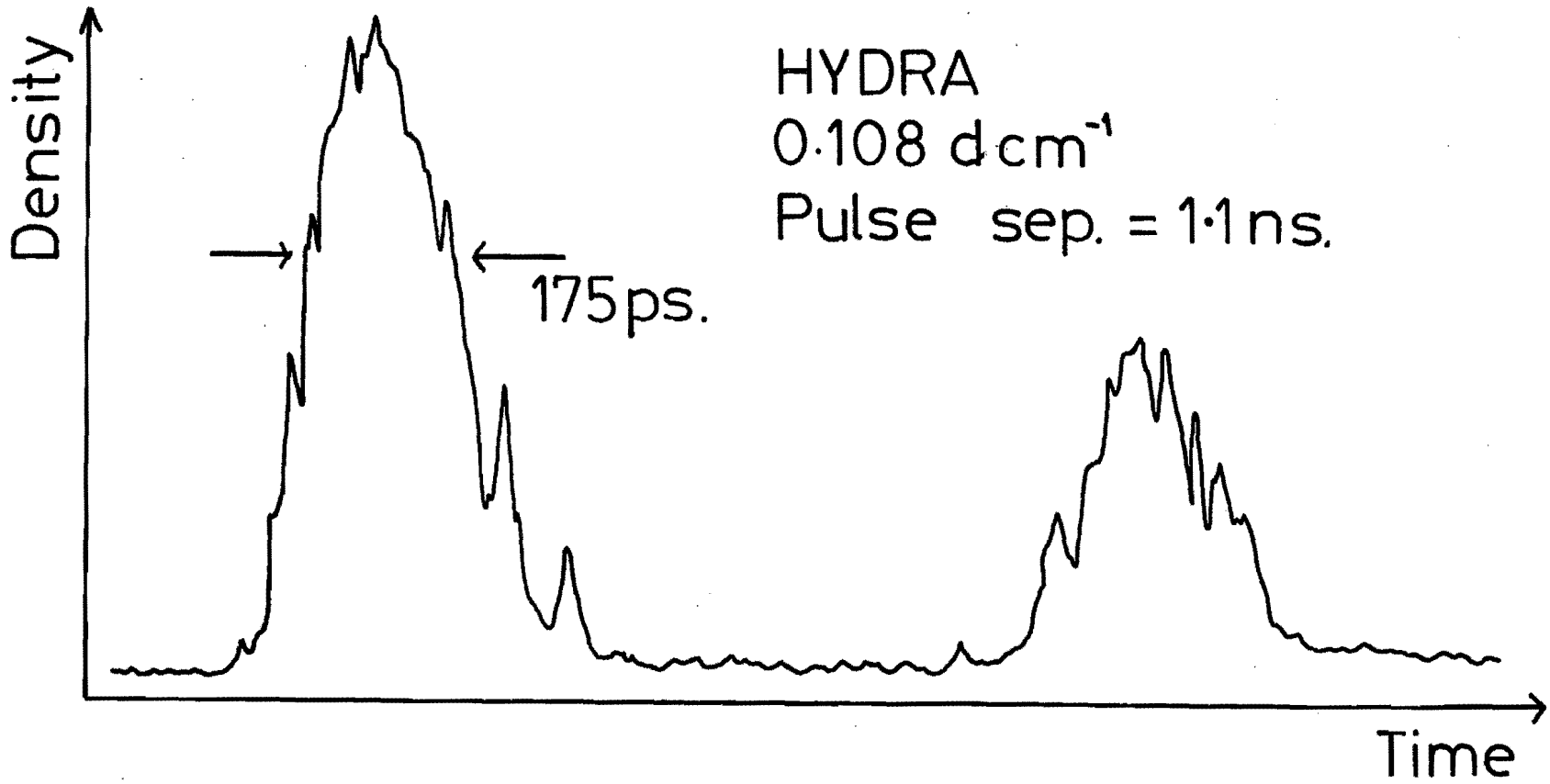

STREAK CAMERA RECORD OF THE HYDRA OUTPUT
FIGURE 11

Use of an Interference Edge Filter Output Coupler

In an attempt to balance the output energies of the two wavelengths from the oscillator and increase the stability of the prelase a different cavity configuration was investigated, shown in Figure 7 (cavity (c)). The efficiency (output power / input power) of Nd:YAG is approximately twice that of Nd:YLF. To compensate for this the conventional broadband cavity output mirror M_1 was replaced by an interference edge filter, (designed and supplied by Dr AK Roy of Queens University, Belfast) whose transmission profile compensates for the efficiency difference between the two wavelengths.

At lasing threshold (3.5):

$$\text{Pump energy (E)} = \frac{\ln G}{\sigma K} = \frac{-1}{\sigma K}\left(\ln T + \ln R_1 R_2 \right) \qquad 3.7$$

where; G is the single pass amplifier gain, R_1 and R_2 are the mirror reflectivities, T is the single pass transmission of the cavity components, σ is the cross section and K is a measure of pumping efficiency.

For a simple cavity T = 1.0 and R_2 = 1.0 for both wavelengths.

Also $$(\sigma K)_{1.053} / (\sigma K)_{1.064} = 0.45 \pm 0.04 \qquad 3.8$$

from 3.7 and 3.8 $$\ln R_{1.053} / \ln R_{1.064} = 0.45 \qquad 3.9$$

Assuming a reflectivity of 30% for Nd:YAG at 1.064 microns, equation 3.9 gives a reflectivity for Nd:YLF at 1.053 microns of 58%. At the time of specification the ratio of the line efficiencies (equation 3.8) was not available, therefore the filter was specified purely on experimental experience. The specification of the filter was 30%R at 1.064 microns and 80%R at 1.053 microns at normal incidence. The effect

of this when inserted into the cavity was to change the relative Q-switch envelope heights to 40% at 1.053 microns and 60% at 1.064 microns.

Unfortunately it was impossible to achieve any prelase stability with this reflector. A phenomenon which could not be comprehensively investigated because of limitations in experimental time. Therefore the cavity was returned to the configuration (b) in Figure 7.

Diagnosis using a Streaked Spectrometer Output

When the Hydra oscillator was used in the system trial experiment a spectrometer was added at the input to the streak-camera. A fraction of the laser beam was split off at the output of the system. This beam was aligned through a spectrometer whose output was incident on the streak camera. This provided a more accurate method of determining the wavelength synchronisation than with a streak-camera alone as described above. At the input to the streak camera an etalon was set up to produce multiple pulses of known temporal separation to provide an accurate streak calibration. A streak record of the two wavelengths is shown in Plate 7. The two pulses were not exactly synchronised. To ensure that this was not caused by dispersion through the system, the output of the oscillators was propagated directly to the spectrometer/streak camera diagnostic. The results of this were identical.

An explanation for the lack of synchronisation between the wavelengths is the competition within the cavity, as mentioned previously, between the 1.053 micron wavelength in Nd:YLF and the 1.052 micron line in Nd:YAG which shares a common upper state lasing level with the required 1.064 micron output. Additionally the dispersion within the cavity between the two wavelengths may produce round trip time discrepancies, resulting in inter-pulse variations. First order calculations had shown that the dispersion through the cavity would not cause a problem, but good data was not available for all components.

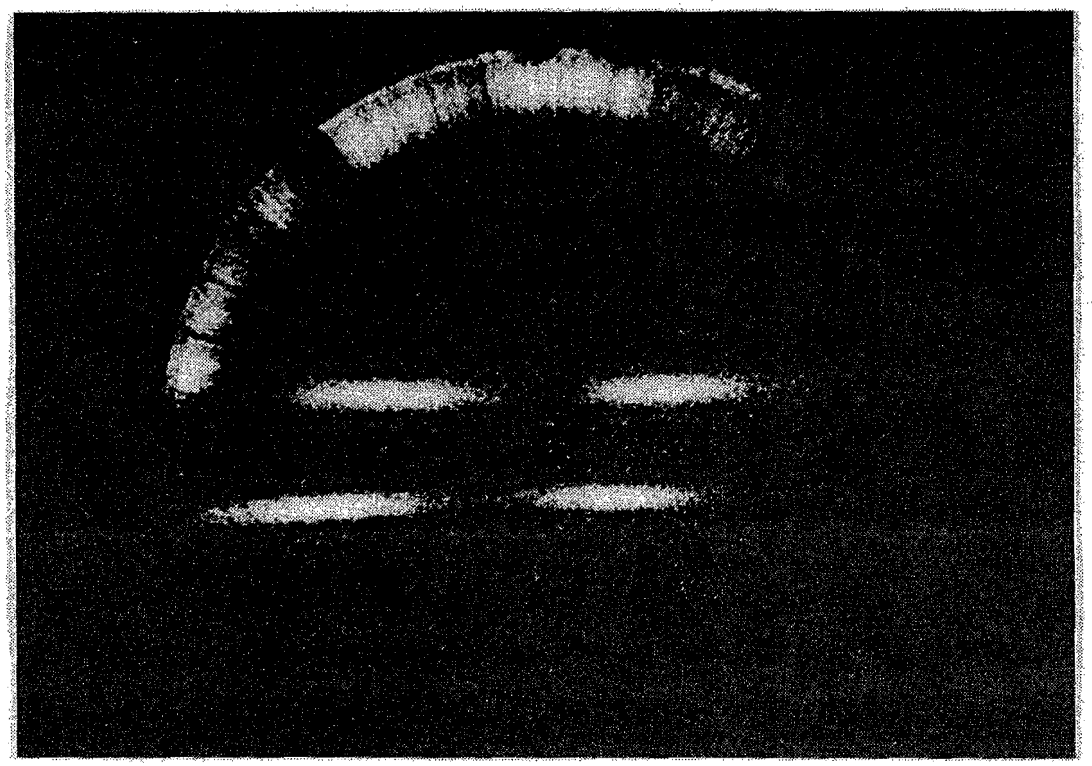

STREAKED - SPECTROMETER OUTPUT
OF THE HYDRA OSCILLATOR
PLATE 7

Conclusion

The Hydra oscillator system was used in a trial experiment to verify whether the VULCAN laser system could produce the required energies for the experiment. The oscillator proved that the design of the system was adequate, but that it would prove impractical to use the oscillator system in target experiments. This was because the pulses were partially asynchronous and the reliability from shot to shot was poor. It was therefore necessary to design and build a new pulse generation system, described below.

3.3.b Dual Cavity Operation

To alleviate the stability problems encountered with the Hydra oscillator the oscillator system was redesigned, with two separate cavities linked by the same control electronics. In this way it was possible to generate the two pulses necessary for the experiment but with increased stability.

Temporal Pulse Control

A schematic of the optical and electronic layout of the oscillator is shown in figure 12. The design of each cavity was the same as used for the Hydra system, but the Nd: YAG and Nd:YLF rods were mounted in optically decoupled cavities.
A fixed temporal relationship between the output pulses of the two oscillators was ensured, using three levels of control.

(i) An external trigger, derived from the sync-timer unit in the main control room, was sent to both oscillator power supplies. This enabled the oscillator outputs to be synchronised to the rod and disc amplifier firing to within 10 μs.

(ii) The oscillators were operated in a stable prelase mode as with the Hydra cavity. In this mode of operation the Q-switch envelope, generated when the cavities were switched from a low Q to a high Q state, had build-up times which were consistent from shot to shot, with a jitter of about 5ns. The triggers to the two Q-switch units were obtained from the same source, the relative timing could be adjusted using the cable delay ΔT_2 (fig 12).

(iii) To enable synchronisation of the individual pulses the optical round trip times of the two cavities had to be equal, therefore it was necessary to operate the two mode-lockers at the same modulation frequency. This required a single r.f. voltage generator to be used with the signal divided in an r.f. splitter. A pair of matched mode-lockers were used whose resonant

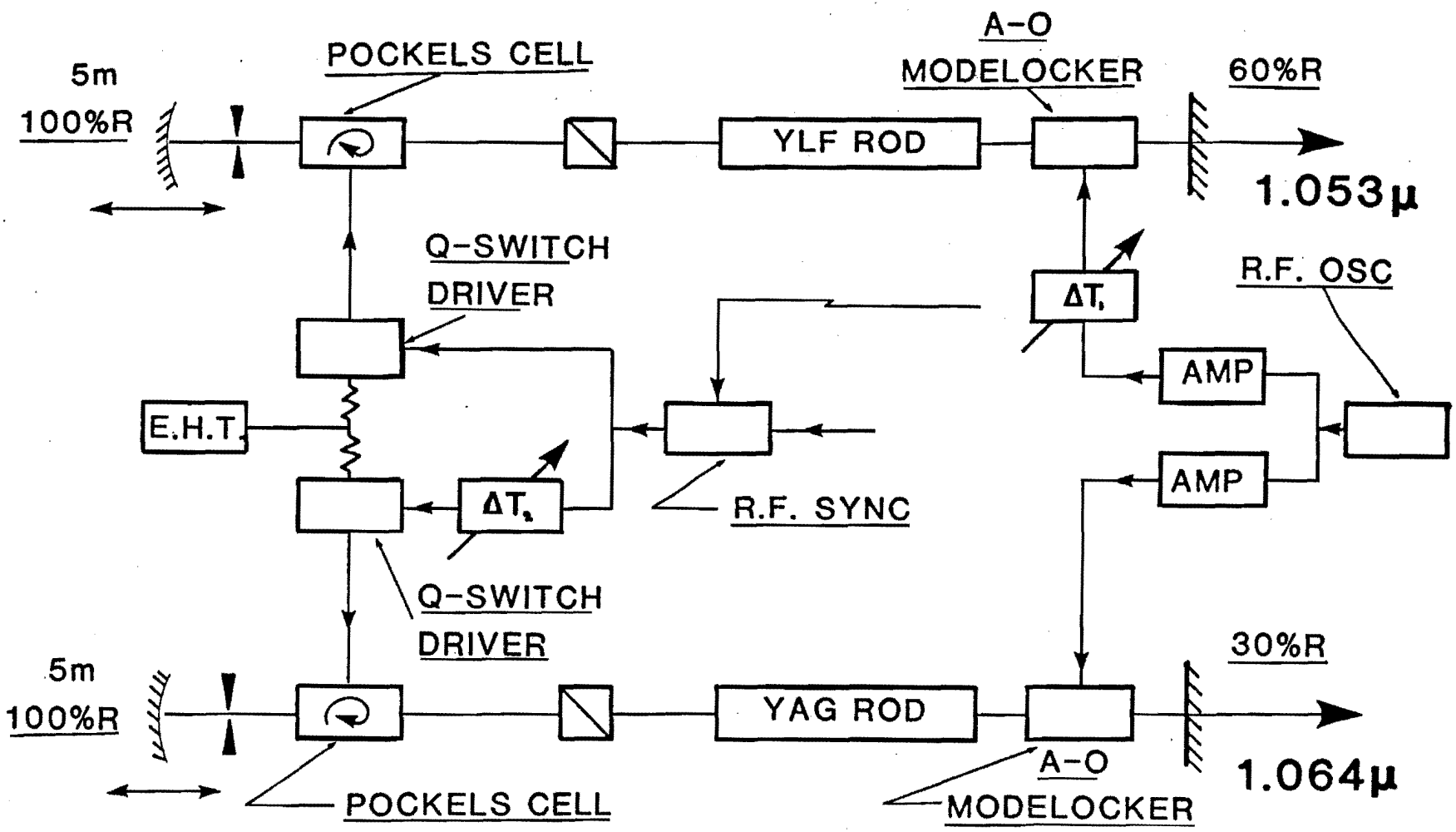

DUAL CAVITY OSCILLATOR SYSTEM CONFIGURATION
FIGURE 12

frequencies were identical allowing the same temperature stabilised cooler for them both. It was possible to alter the relative timing of the two output pulses by adjusting ΔT_1 (Fig. 12).

Experimental Layout

The layout of the two cavities for the beat-wave experiment in January 1986 is shown in Plate 8. The oscillators were built off-line and installed beside the output disc amplifiers in VULCAN, as shown in the Plate. In the photograph the two high-voltage power supplies can be seen at the back of the optical table. The control electronics for the Q-switch and mode-lockers were housed beneath the table. An alignment HeNe was positioned on the far side of the optical bench. Its output was divided with each beam being aligned using decoupling mirrors down the two cavities. The Nd:YAG cavity is shown in the foreground with the Nd:YLF cavity running parallel to it. The components shown in Plate 8 mounted on the optical bench and listed from left to right are: the HeNe alignment mirrors; the high reflecting 5 meter focal length resonator mirrors; the transverse mode controlling apertures; an interlocked safety shutter; the Q-switching Pockels cells; the Glan-Taylor polarisers; the laser heads housing the active media; the mode-locker alignment mirrors; the mode-lockers, the partially transmitting output couplers and finally detectors to monitor the prelase signals from the two cavities.

Optical Outputs

The two oscillators were operated with prelase in exactly the same way as for the Hydra configuration. The two outputs were identical to those as with the Hydra heads running independently, as shown in Plate 3. The Q-switch envelopes generated from the two cavities are shown in Plate 9. The relative heights of the two signals was less important than in the single cavity case as the two outputs could be

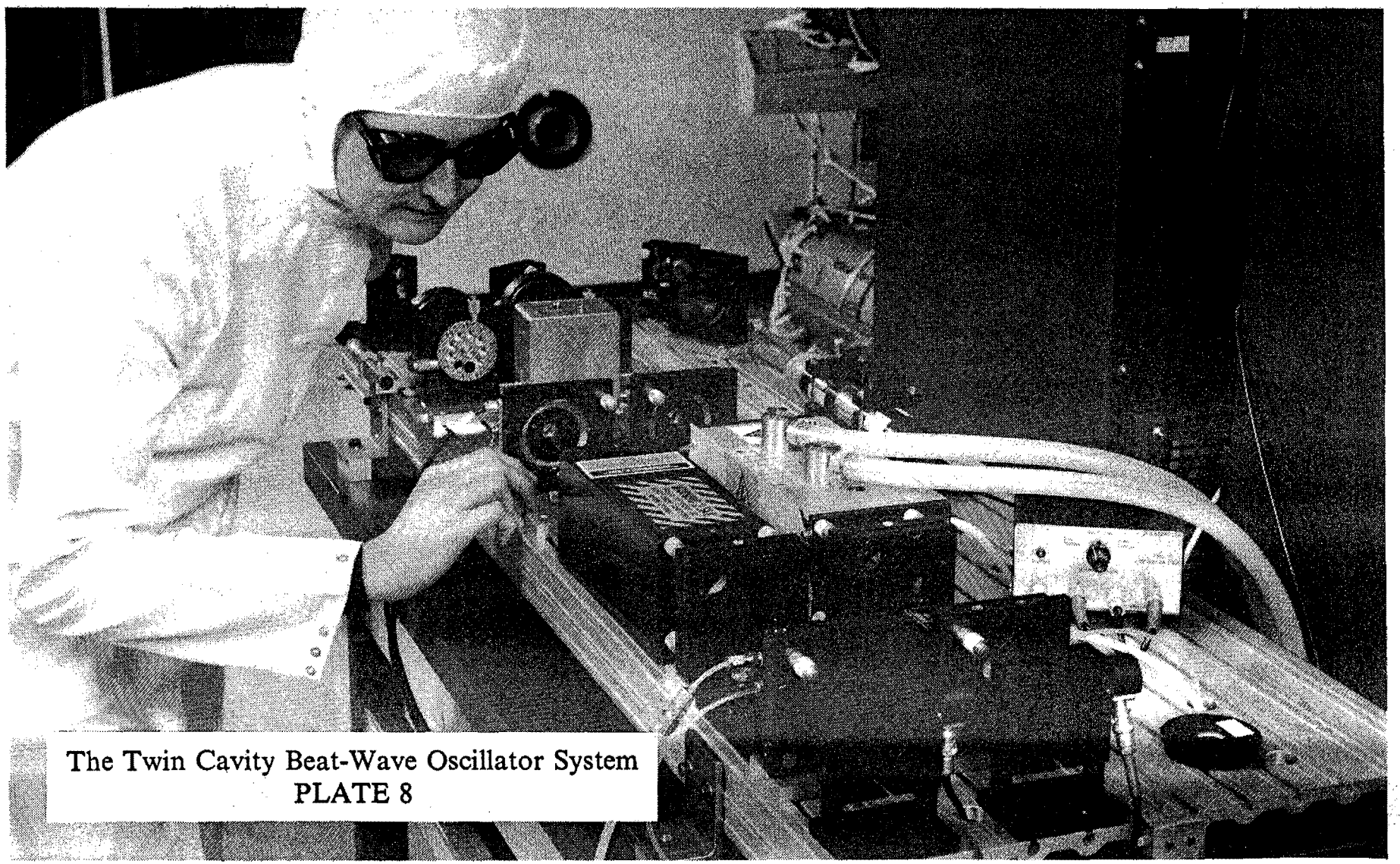

The Twin Cavity Beat-Wave Oscillator System
PLATE 8

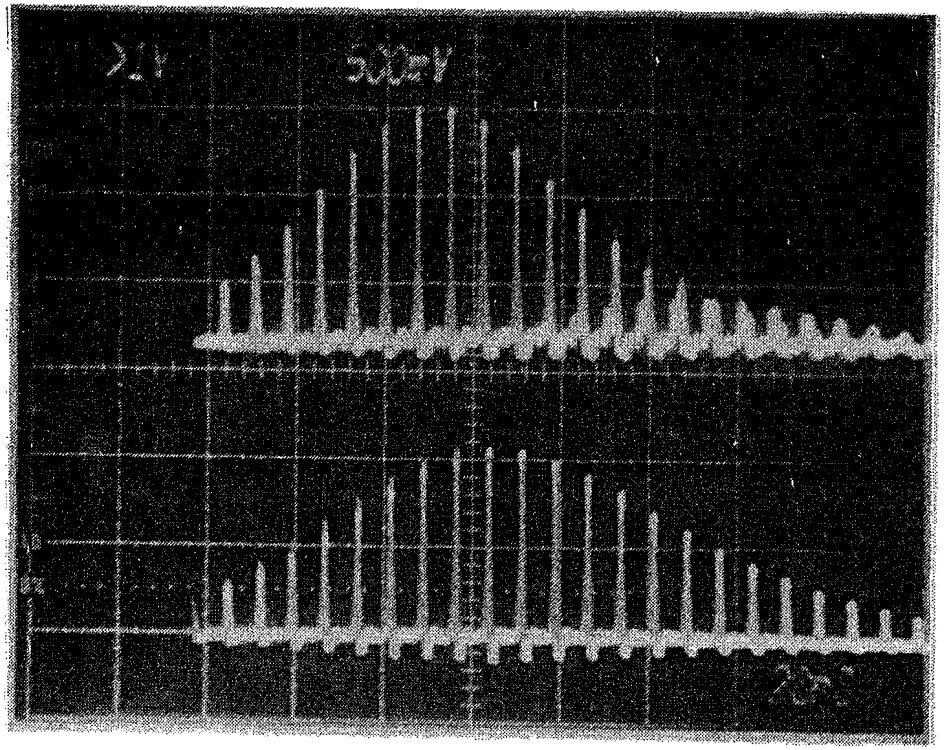

1053 nm

1064 nm

Pulse Separation = 7 ns

PULSE - TRAINS GENERATED FROM THE TWIN CAVITY OSCILLATORS

PLATE 9

attenuated independently to produce the right energy through the amplifier chains.

Pulse Combining

To combine the two pulses at the output of the oscillators a multi-layer dielectric interference filter was developed specifically for this purpose (by Dr AK Roy at the Queens University, Belfast). Using a standard multi-layer dielectric beam-splitter to combine the two pulses would result in a fifty percent loss at each wavelength, making the splitter very inefficient. The specification of the filter was to be highly transmitting at 1.053 microns and highly reflecting at 1.064 microns, both at an angle of incidence of 45 degrees and 'p' polarisation. The measured specification of the delivered splitter was greater than 99 percent reflecting at 1.064 microns and about 75 percent transmitting at 1.053 microns. The efficiency of this device is still better than using a standard 50:50 splitter.

When using multi-layer dielectric interference filters in high powered laser applications damage to the coating is an important factor. With a coating of this type with many coating layers damage levels can be as low as 0.1 joule per square centimetre. At the output of the oscillator the beam fluence was only 0.02 joules per square cm making this type of splitter suitable for the application.

Pulse Synchronisation

Following the beam combiner a single diode can be used to synchronise the two oscillator outputs approximately. The diode output was monitored on a Tektronix 7104 oscilloscope. It was then necessary to adjust the Q-switch delay (ΔT_2 in figure 12) to get the two pulse trains to overlap. To overlap the individual pulses the relative phases of the r.f. voltages to the mode-lockers (ΔT_1 in figure 12) was adjusted. The phase delay was introduced by means of switchable cable delays and an r.f. trombone delay line giving a continuous variation of relative phase delay.

This adjustment is shown in Plate 10. Two r.f. voltage delays to the YAG oscillator are shown, the relative timing difference between the two delays is 3.75 ns.
Using the photo-diode diagnostic it was possible to synchronise the two pulses to about 200 ps. For the experiment it was necessary to synchronise the two pulses to better than 20 ps. To achieve this, part of the beam was split off and was incident on the spectrometer/streak-camera combination described above. Streak camera outputs for two shots are shown in Plate 11. The first trace was with the two pulses asynchronous. The streak rate had been calibrated on a previous shot using an etalon. The second trace shows the two pulses with the trombone delay altered to bring the pulses into synchronisation. The jitter from shot to shot was less than 10 ps; this was within the measuring capability of the streak camera.

Operation for the May 1987 Experiment

During the May 1987 experiment it was necessary to operate with a different configuration. The two wavelengths were propagated down different amplifier chains, this was necessary because of experimental problems encountered in synchronous propagation which will be discussed in the Chapter 4. The output pulses were not combined at the output of the oscillators but combined in the target areas following amplification. It would have proved difficult to propagate the two uncombined beams to the input of the amplifier system from a remote position so the oscillator system was moved under the oscillator covers on VULCAN, shown in Plate 1. This also had benefits as far as stability was concerned as the position is free from air turbulence and does not suffer from large temperature excursions.

Replacement of r.f. Voltage Drive

To produce more stable operation, a different r.f. generator was used for this experiment. The Hewlett Packard tunable supply was replaced by a fixed frequency

R.F. VOLTAGE SIGNALS TO THE TWO MODE-LOCKERS

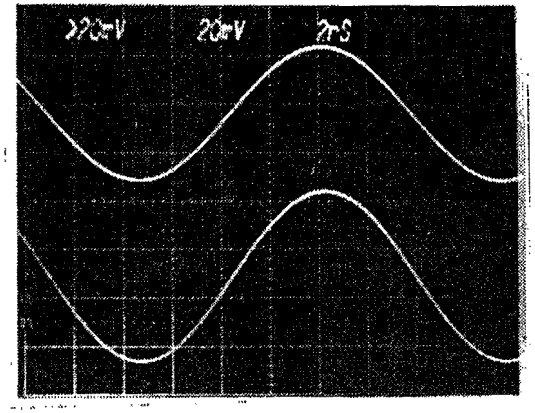

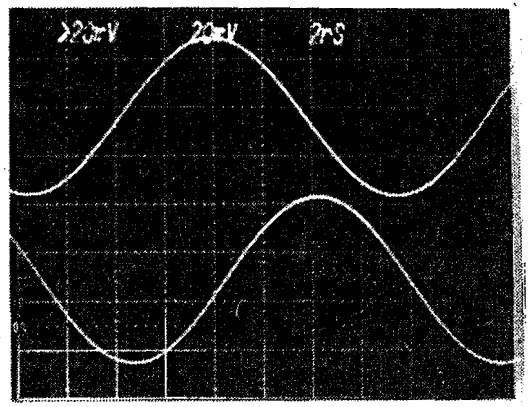

Relative Phase Difference Between
The Two signals = 0 and 3.75 ns

PLATE 10

STREAK CAMERA RECORDS OF TWIN CAVITY OUTPUTS

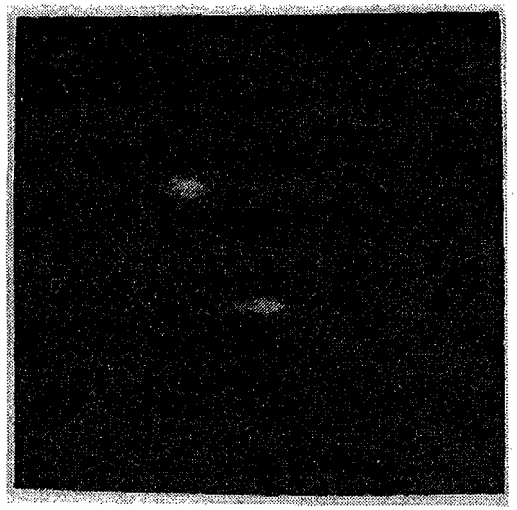

600 ps

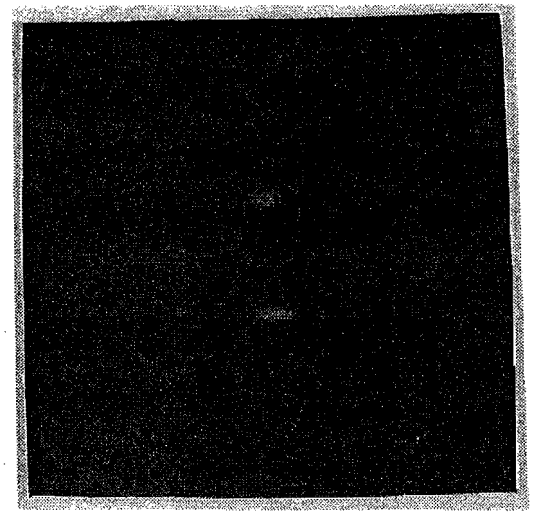

1053 nm

1064 nm

Synchronisation of the Two Pulses Using the r.f. Voltage Phase Delay

PLATE 11

crystal oscillator.

One of the mode-lockers was replaced due to a detached transducer. The replacement had a slightly different resonant frequency. This required the temperature of the mode-lockers to be independently adjusted to be resonant with the applied r.f. To find the tuning range of the mode-lockers the Hewlett Packard r.f. generator was coupled to each mode-locker in turn. An r.f. reflectometer was then connected between the mode-locker and the generator. The temperature of the mode-locker was then scanned. The resonant frequency at each temperature was found by tuning the r.f. generator for a minimum reflected signal. The resonant frequency dependence on temperature is shown in Figure 13, together with the tuning range of the single crystal generator. For this particular mode-locker the operating temperature was 31 degrees C. For the second mode-locker an operating temperature of 24 degrees C was measured.

Monitoring of the Temporal Relationship of the Two Wavelengths

For separate pulse propagation it was no longer necessary to use the spectrometer arrangement to monitor the two individual pulses. The input to the rod amplifiers have a six degree angle normal to the beam direction, and reflections from the front faces of the 16 mm diameter rods were focused into low dispersion, graded index, fibre optic cables. The other end of the fibres were then coupled to a streak camera. The input slit of the streak camera was removed and the fibre ends were positioned in the slit plane. The fibre core diameter chosen was fifty microns, the same as the normal input slit width, producing a temporal resolution of about 3 ps on the fastest sweep rate, resulting in no loss of temporal resolution. The output of the streak camera was imaged onto CCD camera whose output was fed into a frame store. The image could then be analysed using an Apple computer (software supplied by the VULCAN operations group, RAL). A typical streak record generated from this system is shown in figure 14.

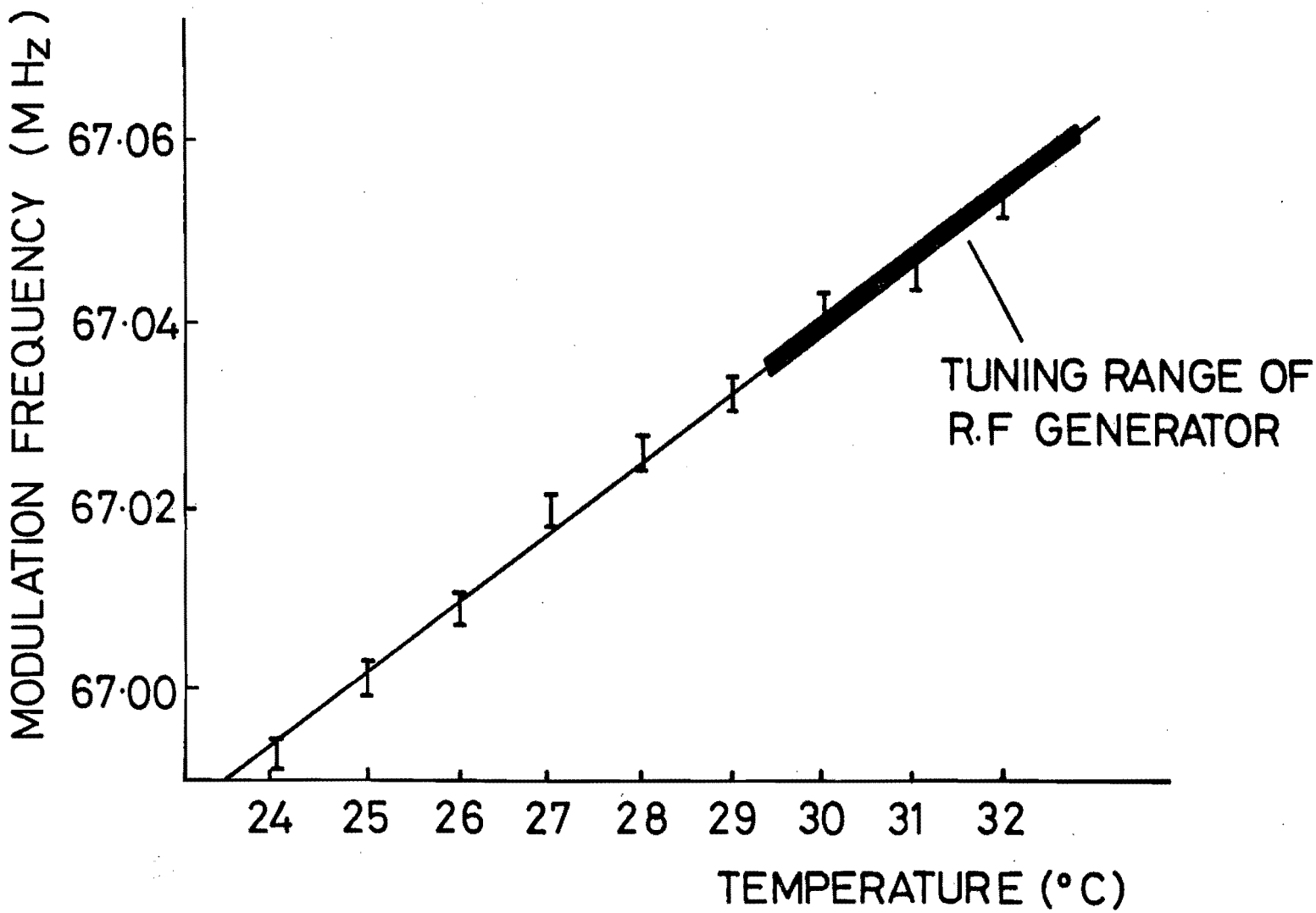

TEMPERATURE TUNING OF THE MODE-LOCKER RESONANCE
FIGURE 13

YAG PULSE LENGTH = 175 ps, STREAK RATE = 40 ps/mm
YLF PULSE LENGTH = 165 ps, STREAK RATE = 40 ps/mm
TIMING DIFFERENCE, YAG TO YLF = -400 ps

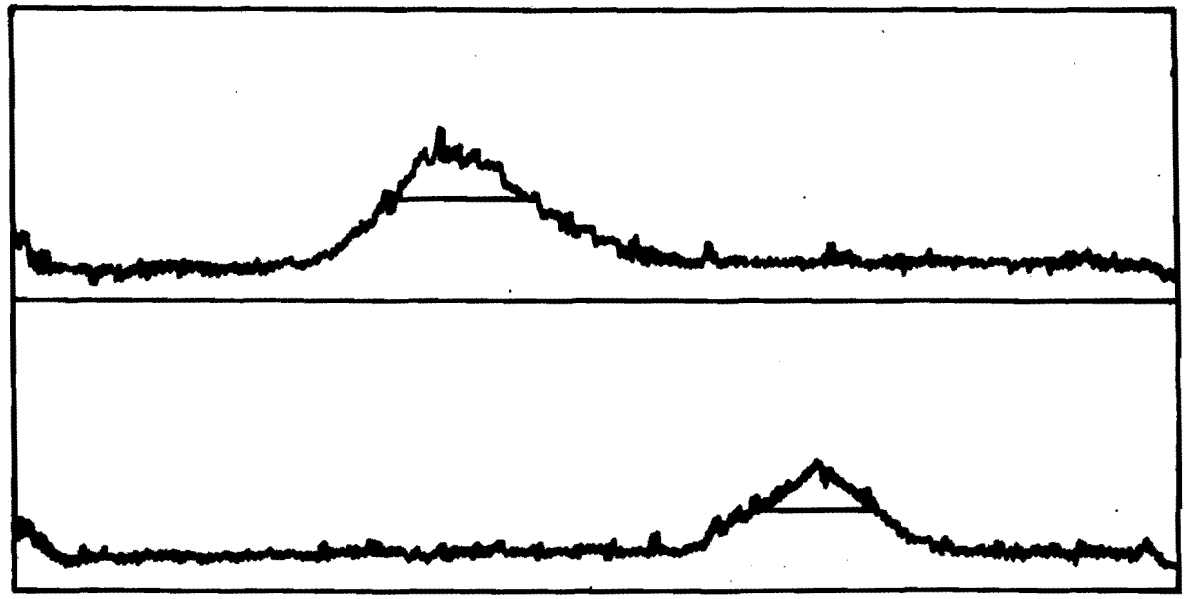

STREAK CAMERA RECORD OF THE DUAL CAVITY OUTPUT
FIGURE 14

Timing Drift Between Oscillator Outputs

When the streak camera output was observed a drift in the relative timing of the two pulses was noticed during course of the day. Despite the drift the shot to shot jitter was still extremely low, well within the measuring capabilities of the monitor. The short term timing drift was compensated for by adjusting the phase difference between the mode-locking r.f. signals (delay ΔT_1 in Figure 12).

One possible explanation of the loss of synchronisation between the pulses was a relative thermal drift of the mode-lockers. To investigate this a number of thermo-couples were positioned to monitor the temperature of the cooling water to both laser heads, the mode-locker temperatures and the room temperature. The drift in timing of the two oscillators was also monitored using the streak camera diagnostic. The results of the investigation are shown in graphical form in figure 15.

During the course of the investigation the room temperature remained constant whilst the relative timing of the two oscillator output pulses drifted by about 500 ps. As the coolers to the laser heads were first switched on they both rose rapidly in temperature towards the operating temperatures of 33 degrees. The temperature of the Nd:YLF cooler stabilised in about 90 minutes whilst the Nd:YAG cooler took about 7 hours. It proved impossible to take relative timing measurements before 60-90 minutes of operation as both oscillators were too unstable.

The reason for the timing drift with relatively small changes in temperature is believed to be attributed to a change in the resonant condition of the mode-lockers. Following the seven hour stabilisation period it was possible to achieve good temporal stability between the two wavelengths. It was found that the different stabilisation times could be attributed to different rates of cooling flow between the two supplies. By modification of the secondary cooling flow the problem was solved.

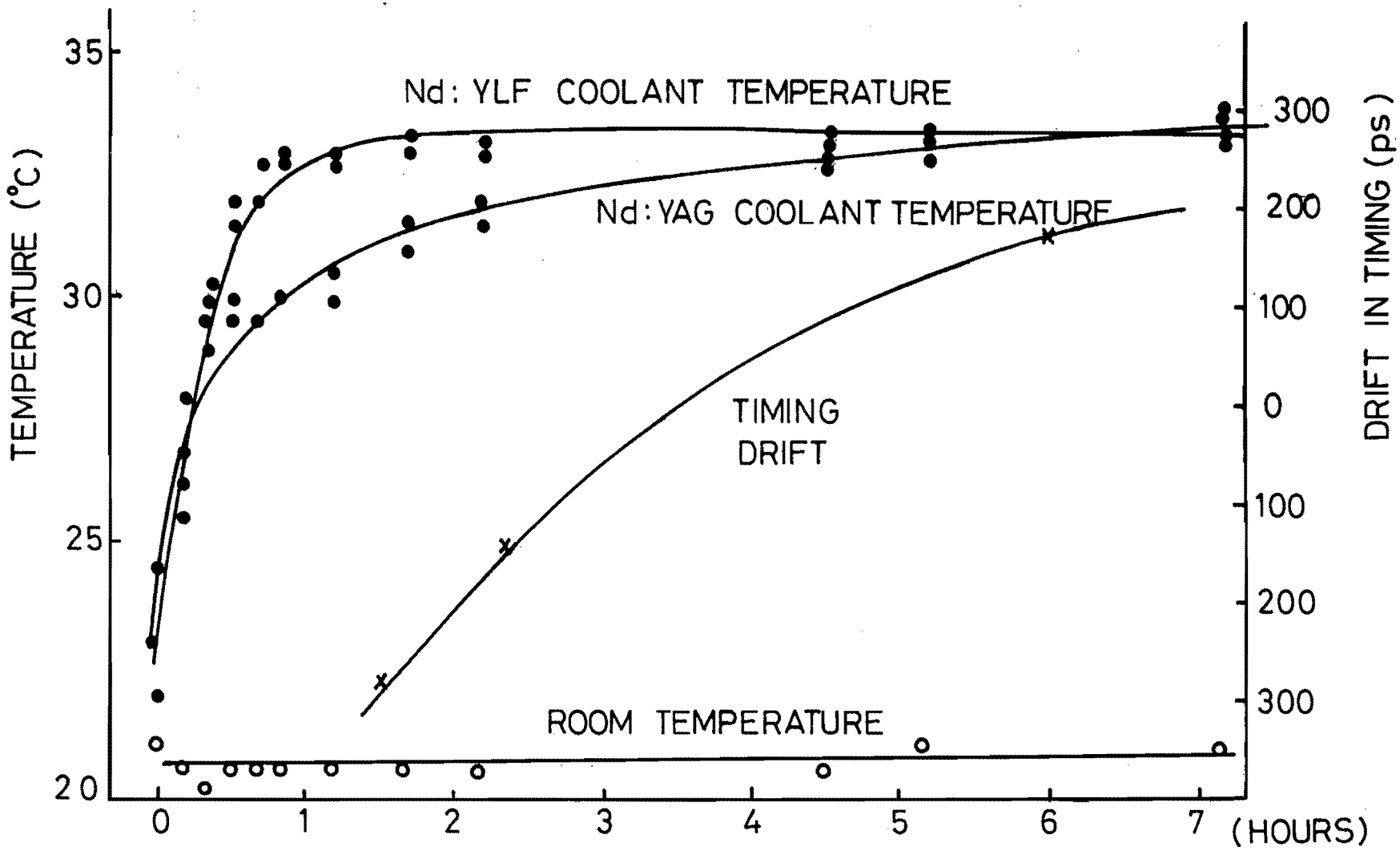

INVESTIGATION OF THE TIMING DRIFT PROBLEMS
FIGURE 15

Conclusion

The oscillator system described above has been used in three different Beat-Wave experiments (January 1986, April 1987 and August 1988). In each experiment the oscillators worked reliably with only minor problems. This final design of pulse generation system will be used in any future experiments.

CHAPTER 4

VULCAN GAIN STAGING FOR THE BEAT-WAVE EXPERIMENT

Abstract

In this chapter are described the design, development and commissioning of the gain staging to generate sufficient laser power for the Beat-wave experiment and the measurement technique employed to determine the amplifier gains at the two relevant wavelengths.

4.1 Introduction

Having generated the two pulses at the appropriate wavelengths and pulsewidths, the next stage in Beat-wave development was the amplification of the pulses to the appropriate energies. The experiment required the maximum energies possible from the VULCAN system. This limits the energies to about 80 - 100 Joules for each beam dependent on the pulsewidth and configuration used. The phosphate glass laser medium exhibits different gain at the two wavelengths therefore it was necessary to reconfigure the VULCAN amplifier chains to balance the output energy at the two wavelengths.

For the experiment the pulses were required to be synchronous, spatially coincident and maintain a good phase relationship. In the original Beat-wave experiment, the two pulses were propagated in the same amplifier chain. The temporal relationship was set by the oscillators. Spatial coincidence was automatically achieved through alignment procedures at the input to the system. As the beams were propagated together any phase irregularities on one beam was about identical on the other.

When the two pulses were propagated down separate amplifier chains the temporal coincidence was again set by the oscillators, monitored by observing the pulses on a

target area diagnostic. The spatial coincidence was achieved by precise near-field and far-field target alignment and a good phase relationship was maintained by effective spatial filtering of the beams to limit beam break-up, described later.

4.2 Gain Staging Design Criteria

To design a suitable reconfiguration to the VULCAN laser system there are several criterion that need to be taken into account. The most important of these are summarised below.

(i) Gain Requirement

The energy of the pulses as they exit the oscillator/switchout system is about 100 micro-Joules. To provide the required energy a system gain of about one million was required. In the normal configuration there is sufficient gain for the 1.053 micron output, but at 1.064 micron, there would only be a gain of about ten thousand. In order to balance the gain at the two wavelengths, two glasses, phosphate and silicate, having different stimulated emission cross sections were used in the system. The gain coefficients of the phosphate and silicate glasses, in the wavelength range of interest, is shown in Figure 16. The 1.064 micron line has the same gain in both media, although there is strong discrimination on the 1.053 micron line. The relative gains of the two wavelengths in the two media were either measured or calculated, the results are presented in section 4.3.

(ii) Component Damage

The energy density limit is set by laser induced damage to optical components. The most sensitive components are the multi-layer dielectric coatings on mirrors and polarisers. Typical damage levels for these coatings is about 5 Joules per square

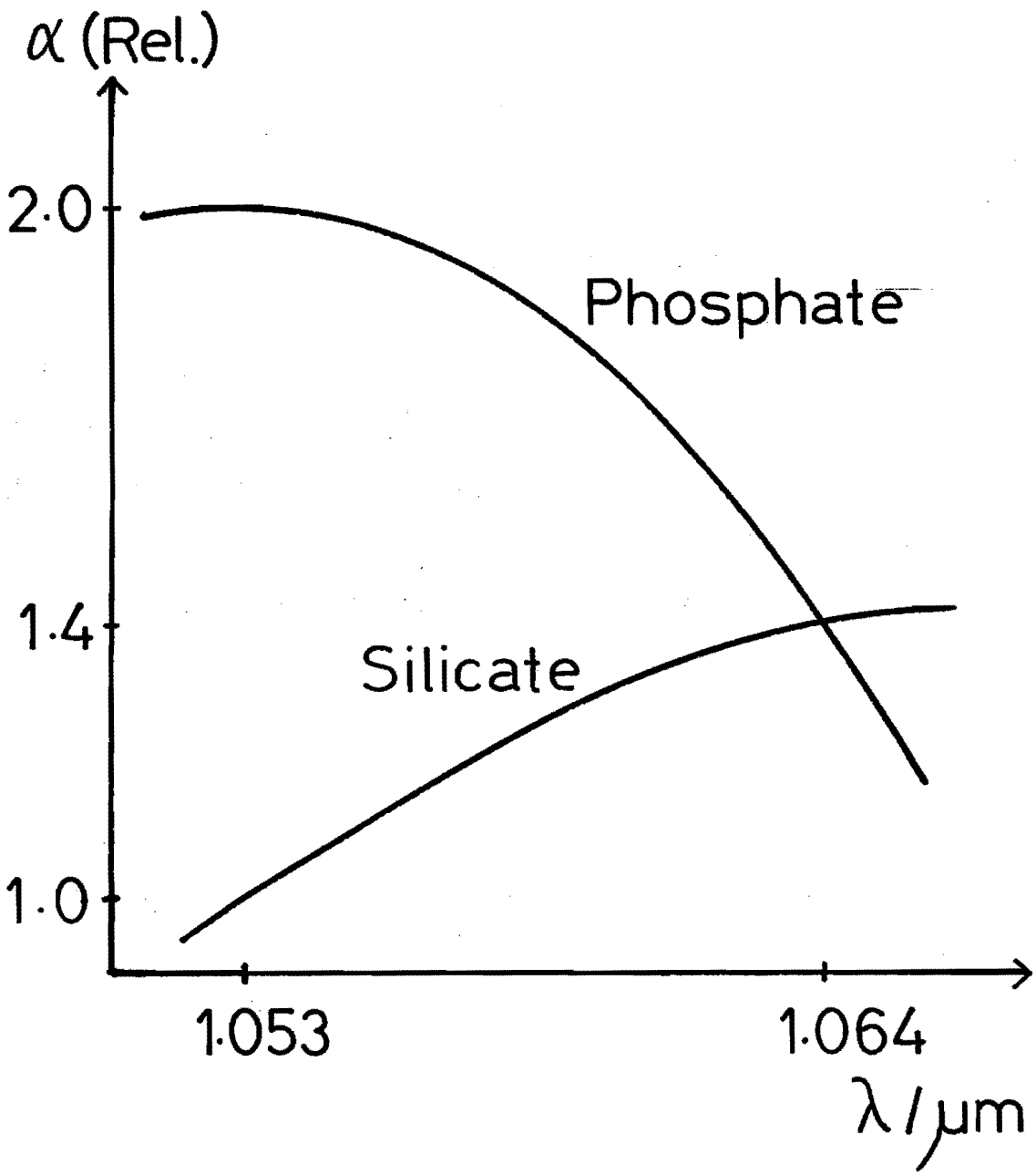

GAIN COEFFICIENTS OF SILICATE
AND PHOSPHATE LASER GLASSES
FIGURE 16

centimetre. To prevent component damage the peak laser fluence was kept below this value.

(iii) Small Scale Self Focussing

The spatial variation of energy density in the beam can be affected by the onset of non-linear optical processes. The most important of these processes is small-scale self-focussing (SSSF). An intense laser beam propagating in a media induces an increase in the refractive index proportional to its intensity. Large aperture laser beams have amplitude irregularities across them caused by diffraction from dust particles, damage in optical components and clipping at beam apertures. When this beam passes through a non-linear medium, such as a laser glass or crystal, it tends to break up into small filaments due to the SSSF.

This phenomenon can be described by the intensity-dependent phase retardation, (B) which is given by (4.1)

$$B = 2\pi/\lambda \int \gamma I(z)dz \qquad 4.1$$

where; λ is the operating wavelength and γ is the non-linear refractive index. The difference in refractive index produces a variation of phase across the beam. The B-integral gives the phase difference between the low and high intensity parts of the beam. It has been shown that of any intensity ripples on the beam grow at a rate of

$$G = e^{B} \qquad 4.2$$

In practical systems it is therefore necessary to keep the value of B to less than 3 or 4 to prevent the beam from breaking up.

This effect can increase local energy densities severely, resulting in possible component damage problems. To control the growth of these filaments, spatial filtration of the beam is necessary. If a lens is used to focus the beam, the high

spatial frequencies contained within the filaments fall outside the main focal region. If a pinhole is placed in the focal plane it is therefore possible to remove the high spatial frequencies associated with the filaments. The beam is then re-collimated by a second lens.

(iv) System Isolation

In laser systems consisting of many amplifiers it is necessary to provide isolation between amplifying stages. The main reasons for this are:

(a) To prevent spontaneous emission from amplifiers at an early stage in the system being amplified through the system causing possible damage to the target.

(b) To prevent pulses being reflected back down the amplifier chain causing damage to components at the input to the system.

(c) To prevent the amplified spontaneous emission depleting the gain of amplifiers prior to the arrival of the oscillator pulse.

One method commonly used for isolation is the use of Pockel cells. A crystal suitably orientated is placed between crossed polarisers. Under the influence of an external electrical field the crystal becomes birefringent rotating the plane of polarisation of the transmitted beam. If a short electrical pulse is applied, the Pockel cell acts as an optical gate. Another method of isolation is the use of a Faraday rotator between crossed polarisers, which act in a similar way to electrical diodes; allowing high forward transmission and high attenuation for pulses travelling in the backward direction.

Using these laser design factors and other more practicable criterion such as cost, delivery times of new components and space available for installation it was possible to design configurations suitable for the Beat-wave experiment, described in Section 4.4.

4.3 Amplifier Gain Measurements

The amplifiers used for the experiment were neodymium doped phosphate and silicate glass rods and discs. In order to design the gain staging it was necessary to determine the small signal gains of the amplifiers at both 1.053 and 1.064 microns. Silicate glass amplifiers were not available before the experiment making it impossible to measure their gains. These were calculated using the measured phosphate data and the relative gain coefficients.

Pulse amplification can be described by a set of coupled rate equations, which describe the growth of the population inversion and the radiation density within the laser medium. Solutions to these rate equations have been found (4.2), and can be written in terms of the measurable laser parameters to describe the energy of the pulse as it passes through the amplifier as (4.3)

$$E = E_s \ln \{ 1 + [\exp (E_{in}/E_s) - 1] \exp \alpha l \} \qquad 4.3$$

where; E_s is the saturation energy and is the ratio of the energy that can be extracted divided by the small signal gain coefficient αl, E_{in} is the energy into the amplifier and l is the propagation distance through the medium.

If the input energy, E_{in} is much less than the saturation energy then 4.3 simplifies to

$$G = \exp \alpha l \qquad 4.4$$

where G is the small signal gain. From 4.4 it can be seen that as a low energy pulse passes through an amplifier the gain is exponential with length.

Conversely in the heavily saturated regime 4.3 simplifies to

$$G = 1 + (E_s/E_{in}) \alpha l \qquad 4.5$$

As can be seen from 4.5 as a high energy pulse passes through an amplifier the gain is linear with length.

The amplification regime pertinent to the Beat-wave experiment is that given by 4.4 because the experiment requires relatively short pulses of 200 - 300 ps. When operating with short pulses the maximum output energy is limited by non-linear effects, in particular the onset of small scale self focussing, rather than by saturation effects.

The experimental arrangement for the measurement of optical gain in the amplifiers is shown in figure 17. Two c.w. lasers operating at 1.053 and 1.064 microns were available for the tests. One of the c.w. beams was injected into one of the rod amplifier chains on VULCAN. The beam at the output of the chain was then focussed onto a photo-diode and its output displayed on a Tektronix 7104 oscilloscope. The oscilloscope was triggered externally from a "command to fire" signal available from the amplifier power supplies. This ensured that it triggered reliably and not off shot noise.

An optical chopper was placed in the beam at the input to the rod amplifier chain. The chopper was carefully positioned at the focus of the air spatial filter to minimise the rise and fall times of the chopped signal. Any amplified spontaneous emission, generated when firing the amplifiers, falling on the diode would appear as a change in the baseline signal on the scope, with the chopped cw beam superimposed on it. This made it possible to differentiate between the two signals ensuring an accurate gain measurement .

Depending on the gain of the amplifier being tested two different measurement techniques were necessary. For a low gain amplifier, the 'passive' chopped signal and the 'active' chopped signal (when the amplifier was fired) were of similar magnitudes. This made it possible to measure the two signals from the same oscilloscope trace. For a high gain amplifier the active and passive signals were not of the same magnitude. If the oscilloscope was set to measure the active signal the passive signal was too small to be measured accurately. The signal from the photo-

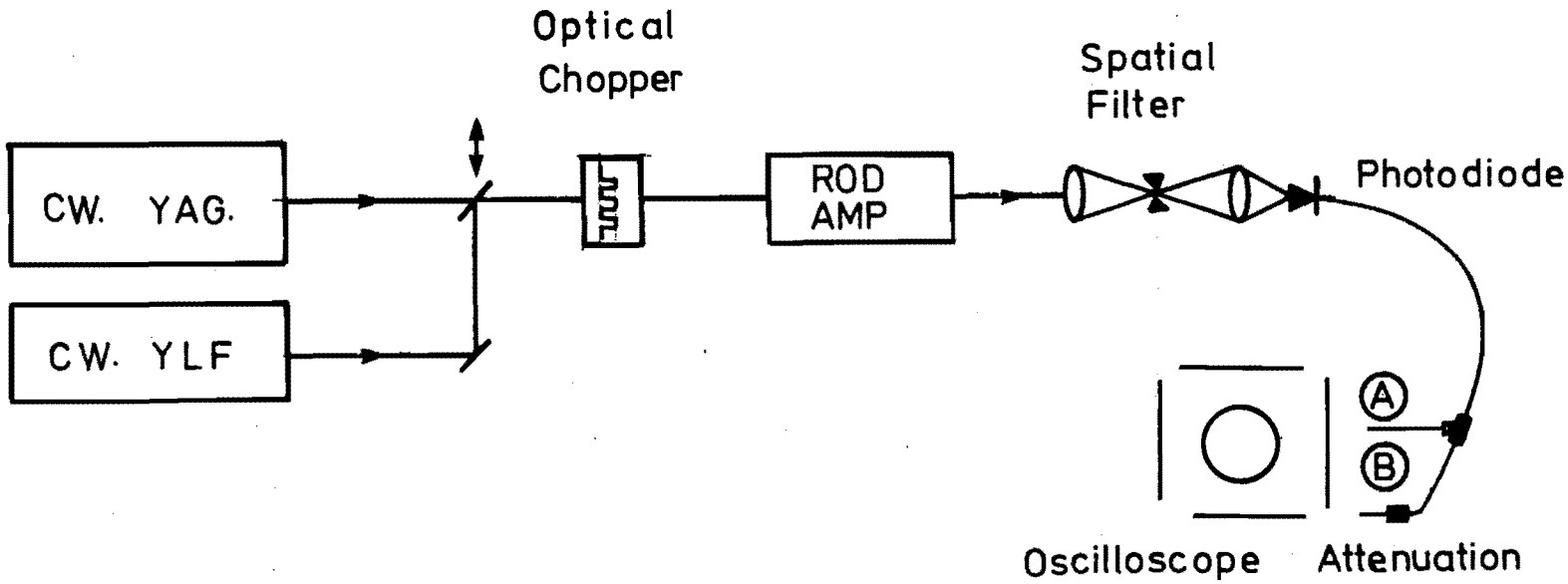

EXPERIMENTAL LAYOUT FOR THE GAIN MEASUREMENTS
FIGURE 17

diode was therefore split, the two outputs put into different channels of the oscilloscope, one channel was set to measure the active signal and the other the passive.

Each amplifier was then fired in turn and its gain calculated from the oscilloscope signals. The experiment was then repeated using the other c.w. oscillator. Typical data obtained from one amplifier is shown in Plate 12. The amplification of the chopped signal can be seen superimposed on a low level of unchopped signal generated by amplified spontaneous emission and fluorescence. The gain of the amplifier was calculated from the ratio of the chopped signal at the peak of the gain to the signal prior to firing. In the case of the 32 mm diameter amplifier shown for example, the gain was calculated to be 3.65 at a flashlamp voltage of 2.2 kV.

The full set of gain measurements of phosphate glass is shown in Table 3, together with the calculated gains in silicate. To balance the energies at the output of the system it would be necessary to modify the gains of the smaller diameter rod amplifiers. As can be seen from the data, the differences in gain are much smaller in the larger diameter rod amplifiers. With this data it was then possible to design the amplifier staging for the two wavelengths described in Section 4.4.

GAIN MEASUREMENTS ON THE 32 mm ROD AMPLIFIER

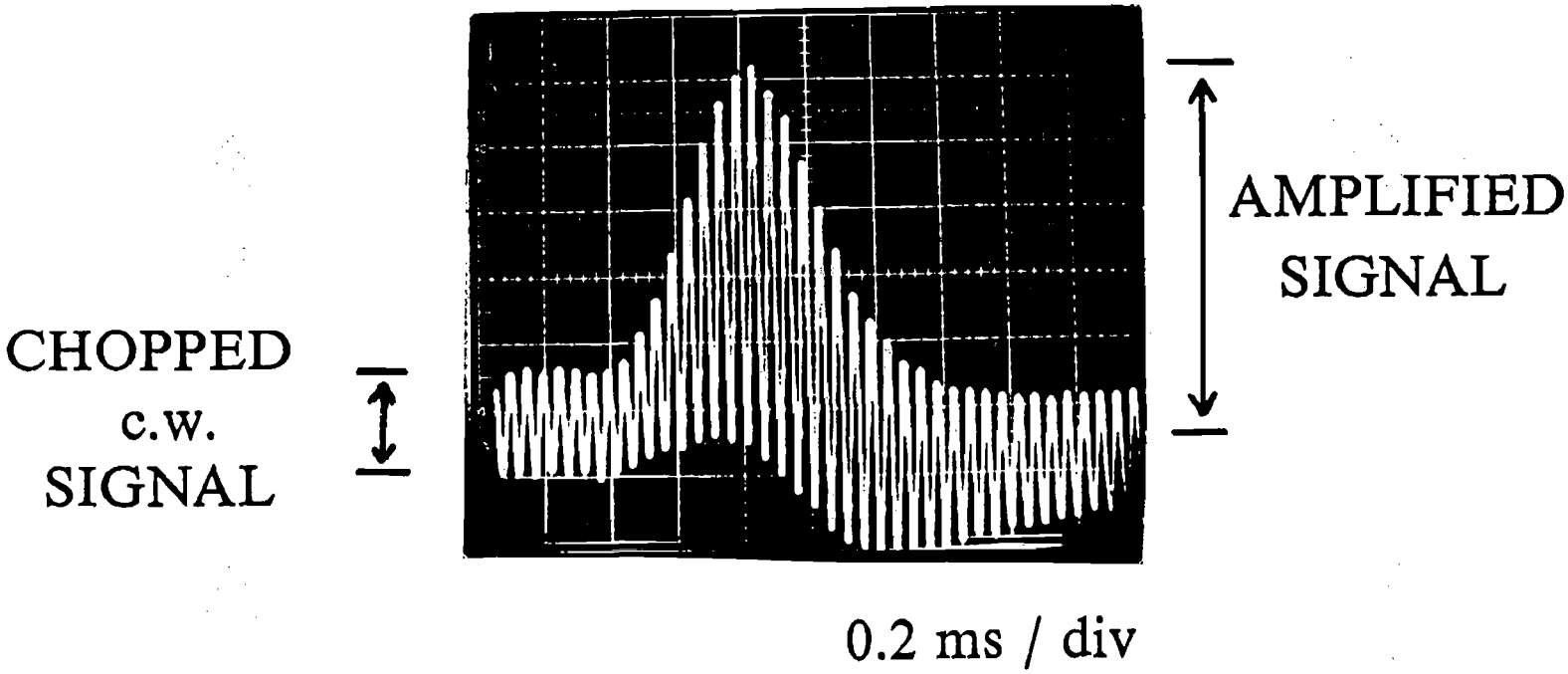

PLATE 12

ROD SIZE mm	PUMP ENERGY kV	PHOSPHATE		SILICATE	
		1053	1064	1053	1064
9	1.8	30	11	5.5	11
	1.6	20	8	4.47	8
16	2.2	23	9	4.8	9
	2.0	19	6.7	3.9	6.7
	1.8	17.5	6.5	3.5	6.5
	1.6	13.3	4.25	2.8	4.25
25	2.2	13.5	6.25	3.7	6.25
	1.9	8.75	5.3	3.3	5.3
	1.7	6.25	4.75	3	4.75
32	2.2	3.65	2.7	2	2.7
	1.9	3	2	1.6	2
45	2.2	2.3	1.7	1.45	1.7
	1.9	2	1.9	1.6	1.9
76	2.2	1.5	1.3	1.2	1.3

ROD GAIN MEASUREMENTS FOR THE BEAT-WAVE EXPERIMENT

TABLE 3

4.4 SYSTEM DESIGN

4.4.a PROPAGATION DOWN THE SAME AMPLIFIER CHAIN

System Configuration

To propagate the two wavelengths in the same amplifier chain it was necessary to use a combination of the silicate and phosphate amplifiers as described in Section 4.2. One immediate constraint on the design was the availability of laser discs in the output disc amplifiers. Silicate discs were unavailable for the experiment and the cost and delivery of getting new ones made this impractical. Using only phosphate discs gives a preferential gain by a factor of eight to the 1.053 micron pulse over the 1.064 micron pulse in the output stages. To compensate for this the gain was balanced in favour of the 1.064 micron pulse through the rod chain by this factor. The staging of the gain for propagation down the same amplifier chain is shown in Figure 18. The oscillator output was injected into a Nd:YAG preamplifier replacing the Nd:YLF preamplifier normally present. The Nd:YAG has a very narrow gain bandwidth compared to the glasses and therefore has a high gain (about 8) at 1.064 microns but has no gain at the 1.053 micron line.

The beam at the output of the pre-amplifier consisted of a train of pulses. To select a single pulse, the pulse-train was passed through three Pockel cells in series, giving an extinction ratio of ten million to one. The Pockel cells were switched using a photoconductive switch device which allowed the synchronous switching of a pulse from the short pulse train and a slice from the long pulse envelope, generating the 1 ns pulse required for Beat-wave diagnostics. The single pulse then passes through a combination of phosphate and silicate amplifiers.

A schematic of the VULCAN configuration in the laser room is shown in Figure 19. The pre-amplifier modifications necessary from the standard configuration were: the second 9 mm diameter amplifier in the chain was changed from phosphate to

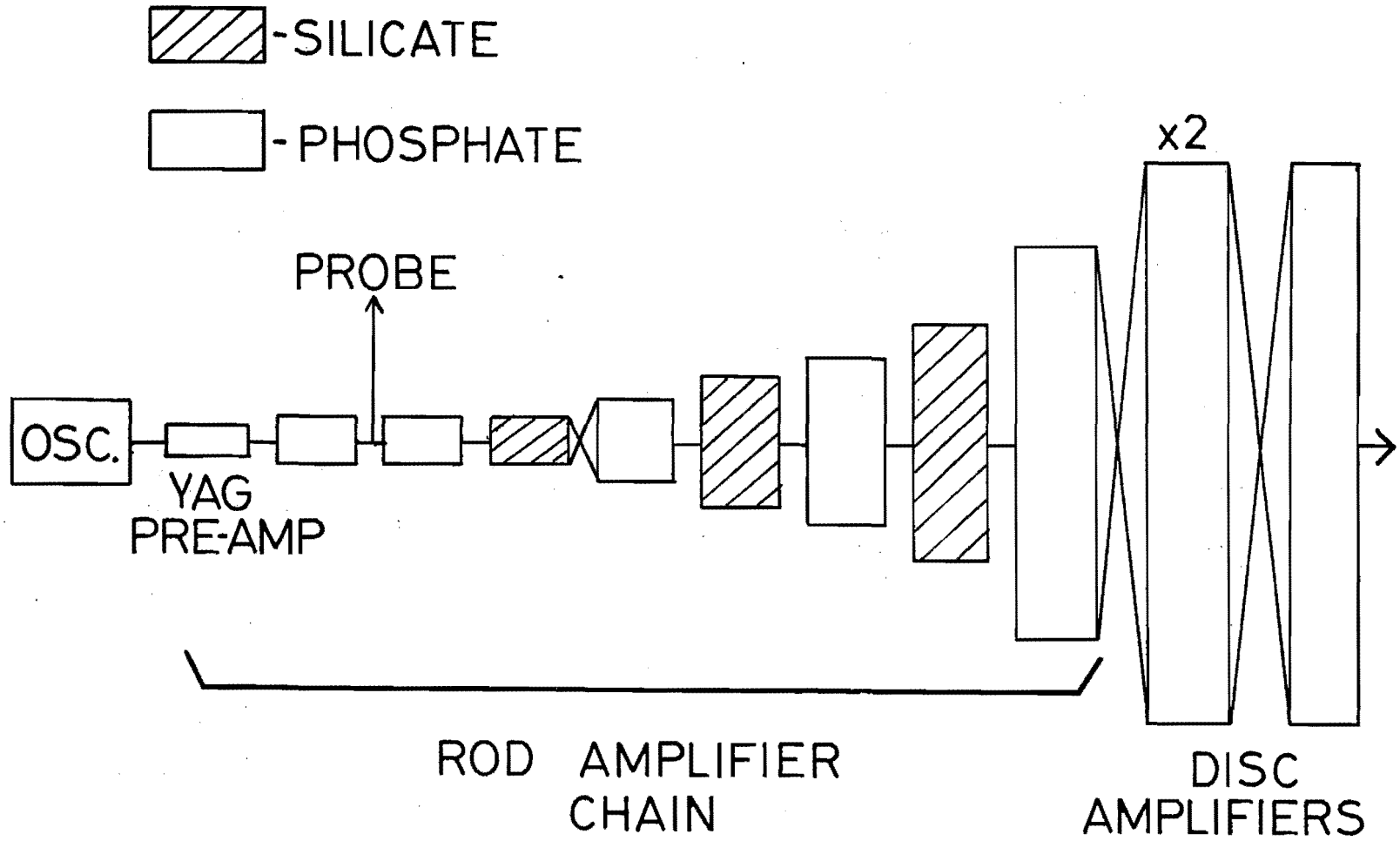

STAGING OF THE LASER GAIN
FIGURE 18

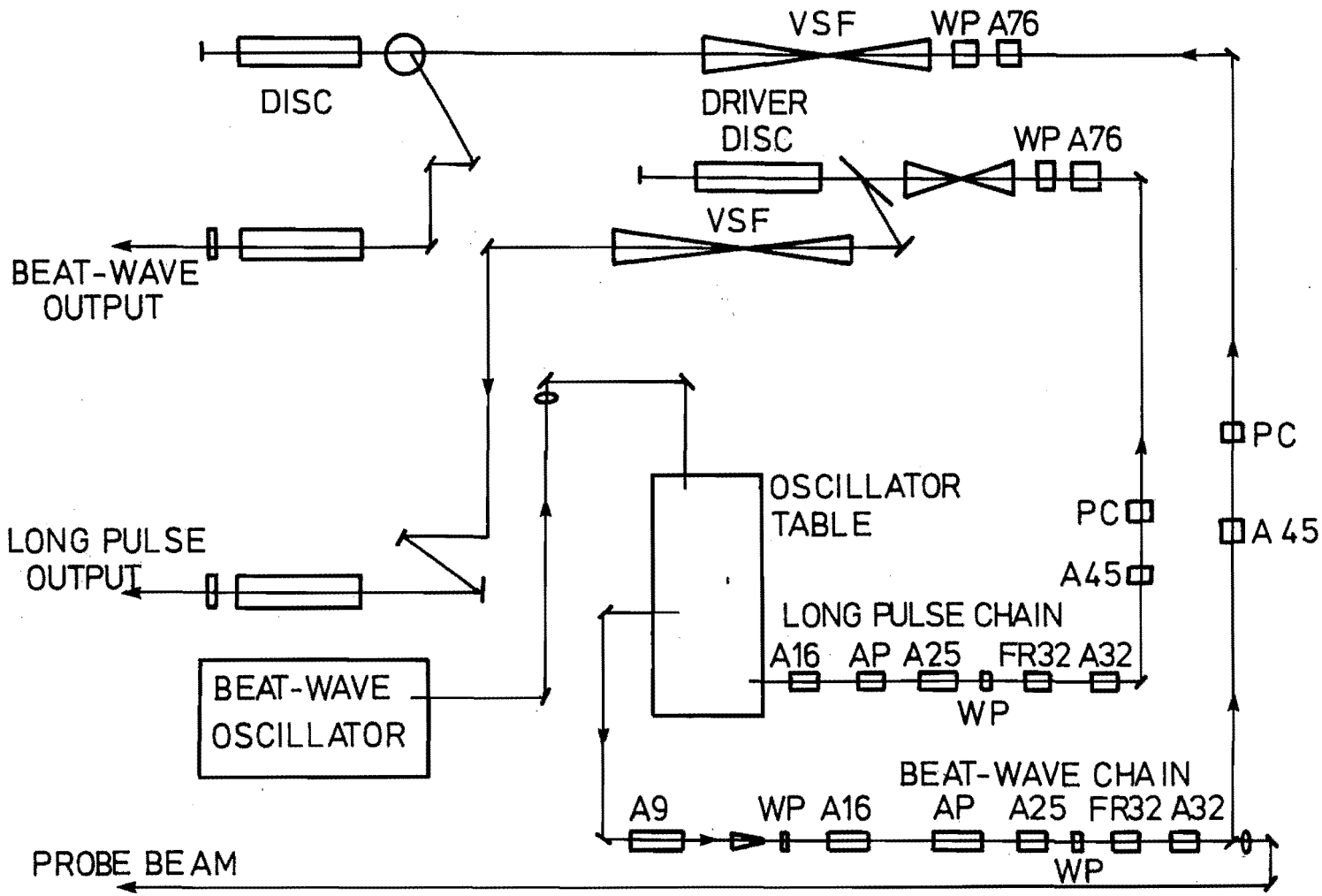

VULCAN CONFIGURATION FOR SYNCHRONOUS PROPAGATION
FIGURE 19

silicate glass and a new 9 mm diameter silicate glass amplifier was introduced. In the main rod amplifier chain the 32 and 45 mm diameter phosphate rods were both changed to silicate. The rest of the amplifier chain, consisting of the 9, 16, 25 and 76 mm diameter rods, was left with phosphate glass. The output stage consists of a double passed phosphate disc amplifier followed by a single passed disc amplifier. This combination of amplifiers gave the required balance in output energies.

The beat-wave interaction pulses were propagated in one rod amplifier chain, while the synchronised long pulse diagnostic beam was amplified in an unmodified amplifier chain. The Beat-wave pulse was then propagated through a double passed disc amplifier and then redirected into one of the disc amplifiers in the normal six beam amplifier array. The long pulse was also propagated through a double-passed disc amplifier before being directed into one of the disc amplifiers in the six beam array.

Calculation of B-integral

To ensure that this design was suitable it was necessary to calculate the B-integral of each stage in the system and as a whole. The B-integral can be calculated using equation 4.1. In the short pulse regime I(z) can be substituted for

$$I(z) = I_o e^{\alpha l} \qquad 4.6$$

and γ can be converted to the standard units of n_o and n_2 using

$$\gamma = 4.19 \times 10^3 \; n_2/n_o \; cm^2/W \qquad 4.7$$

where n_2 is in units of esu.

Using 4.6 and 4.7 and integrating between 0 and l, 4.1 becomes

$$B = 263\ n_2/n_o\ .\ E_{in}/(t_p \lambda A)\ .\ (\ e^{\alpha l} - 1\ )/\alpha \qquad 4.8$$

where; A is the area of the beam and t_p is the pulsewidth. A calculation of B is shown in Table 4 together with the losses and gains experienced by the pulse. It can be seen that in the output stages the value of B reaches a maximum value of 2.47, within the break-up limit of 3 or 4, and the total value of B is 4.21, below the level of 10, which is recommended for high power laser systems.

System performance

The laser system worked well during the first of the beat-wave experiments in January 1986. One problem that did arise was in the alignment of the beams through the rod chains. The system was aligned using a Nd:YLF c.w. laser beam, the pulsed beam was then put onto this path using a nine second repetition rate of the small diameter rod amplifiers. When the rod chain was subsequently fired, to test the beam quality at the rod output stage, low energies were measured and the beam was spatially non-uniform. When the alignment was checked using the c.w. beam and the pulsed beams, no problems were detected.

After investigation the fault was traced to the newly installed nine millimetre diameter silicate rod amplifiers. The beam was monitored at the output of the air spatial-filter as the pulses leave the oscillator pre-amplifier table. When the rods were fired on the nine second cycle the beam was found to deviate at the spatial filter pinhole. Under normal operations, with phosphate glass in the amplifiers, no such problem had been observed. The silicate glass was unable to recover thermally from shot to shot at the high repetition rate.

Referring back to Table 1, the thermal conductivity of silicate glass is actually higher than that of phosphate glass, therefore this did not account for the observations. The problem occurs because of the large difference in the values for the Thermo-optic effect, dn/dT. Any thermal gradients in a rod will result in a

	Gain/Loss 1053	Gain/Loss 1064	Energy 1053	Energy 1064	E_{TOT} (J)	G	L	α	Ø (cm)	A (cm^2)	n	n_2 (10^{-13} esu)	ΔB	B_{TOT}
Pre-Amp Stage			0.0018	0.038	0.04									
Ph A 16 mm	15	6.7	0.027	0.25	0.28	7.04	24	0.081	1.0	0.785	1.51	1.02	0.14	0.14
Waveplate	0.9	0.9	0.025	0.23	0.26									
Apodiser	0.8	0.8	0.020	0.18	0.20									
Ph A 25 mm	8.75	5.3	0.17	0.98	1.15	5.75	24	0.073	2.0	3.14	1.51	1.02	0.15	0.29
Faraday 32	0.9	0.9	0.16	0.88	1.04		5		2.3	4.15	1.68	2.45	0.11	0.40
Si A 32 mm	2.0	2.7	0.31	2.4	2.7	2.6	14	0.068	2.7	5.72	1.56	1.6	0.24	0.64
Si A 45 mm	1.4	1.7	0.44	4.0	4.4	1.63	14	0.035	4.0	12.6	1.56	1.6	0.21	0.85
Pockels Cell	0.9	0.9	0.39	3.6	4.0		5		4.0	12.6	15.	3.56	0.23	1.08
Ph A 76 mm	1.5	1.3	0.59	4.7	5.3	1.33	14	0.020	7.0	38.5	1.51	1.02	0.06	**1.14**
V.S.F.	0.95	0.95	0.56	4.5	5.1									
Polariser	0.95	0.95	0.53	4.2	4.7									
Faraday	0.9	0.9	0.48	3.82	4.3		3		9.5	7.08	1.68	2.45	0.02	0.02
Ph 108 Disc	6	3	2.87	11.47	14.3	3.32	21.5	0.056	9.5	70.8	1.51	1.02	0.09	0.11
Ph 108 Disc	6	3	17.2	34.4	51.6	3.6	21.5	0.060	9.5	70.8	1.51	1.02	0.32	0.43
Faraday	0.9	0.9	15.5	31	46.5		3		9.5	70.8	1.68	2.45	0.17	**0.60**
Polariser	0.95	0.95	14.7	29.5	44.2									
V.S.F	0.95	0.95	14	28	42									
Ph 108 Disc	6	3	84.2	84.2	168.4	4.0	21.5	0.064	9.5	70.8	1.51	2.45	2.47	**2.47**
V.S.F	0.95	0.95	80	80	160									
												TOTAL B		**4.21**

(Pulsewidth = 300 ps)

AMPLIFIER CHAIN COMPONENT PARAMETERS AND B-INTEGRAL CALCULATIONS

TABLE 4

refractive index gradient. This occurs in these rods due to the flashlamp heating and the water cooling producing a radial thermal gradient. The thermo-optic constant for silicate glass is about 20 times larger than for phosphate glass. Therefore although both rods would have about the same thermal loading a problem was only observed when using silicate glass. The problem had not been seen when the pulsed beam was originally aligned because the alignment through the pinhole was found to stabilise after only four or five firings of the rods.

One solution to the problem was to align the beam with the amplifiers 'cold'. That is to fire the amplifiers on a two minute shot rate to allow the silicate amplifiers to stabilise between shots. This method worked well while commissioning the system, but it was recognised that for target area operations the nine second shot cycle was a convenient means of aligning diagnostics. Therefore a second solution for diagnostic alignment was to align and fire the system with the amplifiers 'hot'. This was accomplished on shots by running the nine second cycle during the amplifier charging time prior to the shot (approximately 45 seconds). It was important that full output energy shots were not fired under these conditions. This was because the depolarisation of the beam, caused by the thermally-induced birefringence, produces a non-uniform near-field pattern once the beam was incident on the first polariser in the system.

Operating within these restrictions it was then possible to achieve the required output laser energies of about 80 Joules /beam.

When monitoring the spectral composition of the system output it was discovered that optical side-bands were generated as the two wavelengths propagated through the atmosphere. These are shown in Plate 13. The side-bands were identified as cooperative Raman Scattering from vibrational levels in nitrogen (4.4). The experimental diagnostic of the Beat-wave was via side-band generation and it was found that this atmospheric scattering dominated any signal that may have been present from the beat-wave. It was therefore necessary to redesign the experiment, whereby the beams propagated independently.

A Time Resolved Spectra of the Infrared Pump Beams showing Atmospheric Raman Scattering

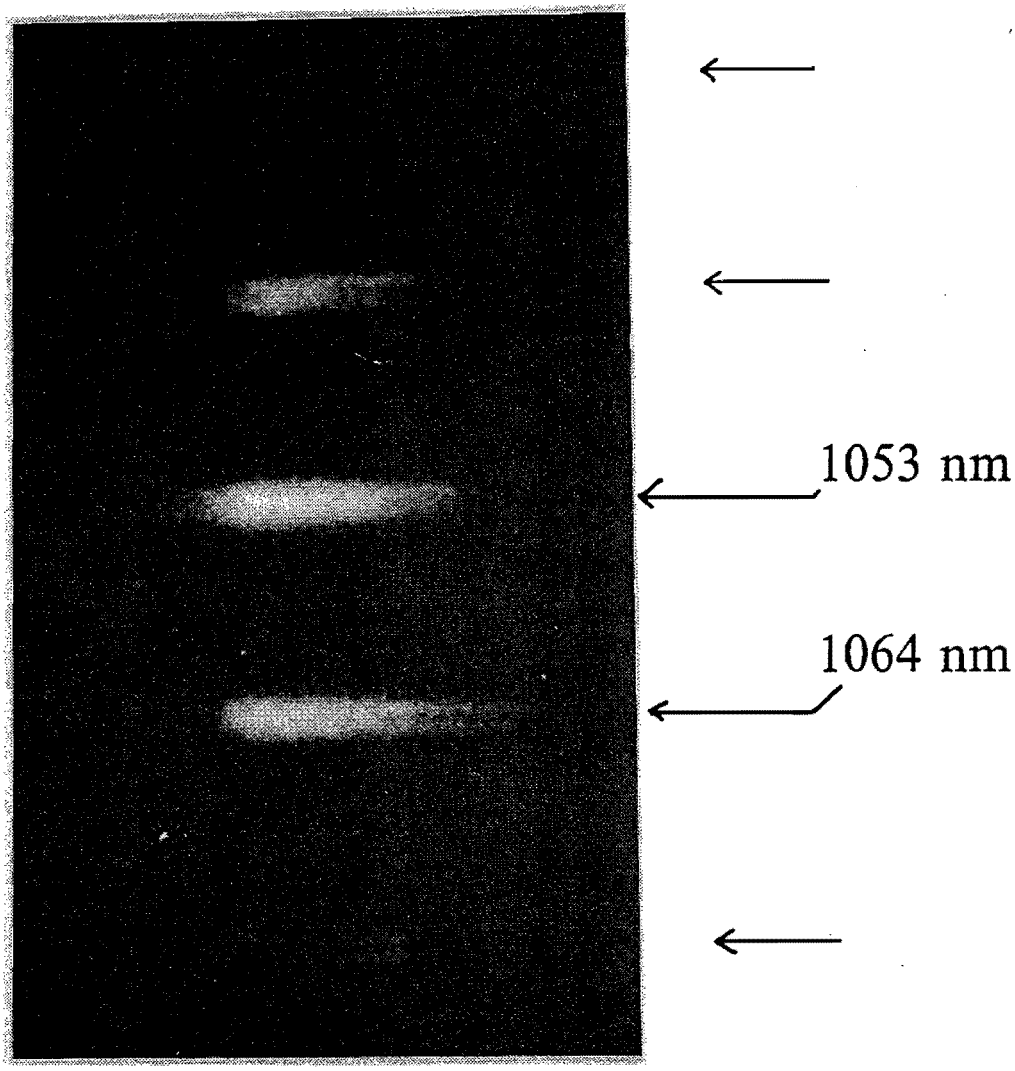

PLATE 13

4.4.b PROPAGATION DOWN SEPARATE AMPLIFIER CHAINS

Introduction

To generate the appropriate pulses for the Beat-wave experiment in May 1987 the two wavelengths were propagated down separate amplifier chains. The oscillators for this experiment were moved under the 'oscillator covers' on VULCAN. This eased alignment of the two pulses into the amplifier chains and provided an environment free from air turbulence. The two beams were then combined in the target area using a novel polariser/waveplate combination in an extension to the vacuum chamber. In propagating the two wavelengths down separate amplifier chains it was no longer possible to generate a long pulse diagnostic beam, although it was possible to deliver other short pulse high power diagnostic beams.

System Configuration

A schematic of the laser configuration is shown in Figure 20. The Nd:YAG pulse was propagated down the same path as for the original Beat-wave configuration, and the Nd:YLF output was propagated down the long pulse chain. With the two pulses propagating down independent rod chains it was not necessary to balance the pulse energy at the output using different amplifying media. The gain of the 1.064 micron beam is the same in phosphate and silicate. It was therefore possible to use phosphate glass throughout, making it much simpler to reconfigure the laser system and to eliminate the thermal problems encountered with silicate.

It was necessary to generate 100 Joules at each wavelength with pulse durations of 200 ps. The amplifier chain for the 1.053 microns needed very little modification from standard operations. Mirrors were inserted at the input to the system to inject the oscillator output into the long pulse amplifier chain and the six beam split at the output of the system was modified to generate a three beam output. This provided

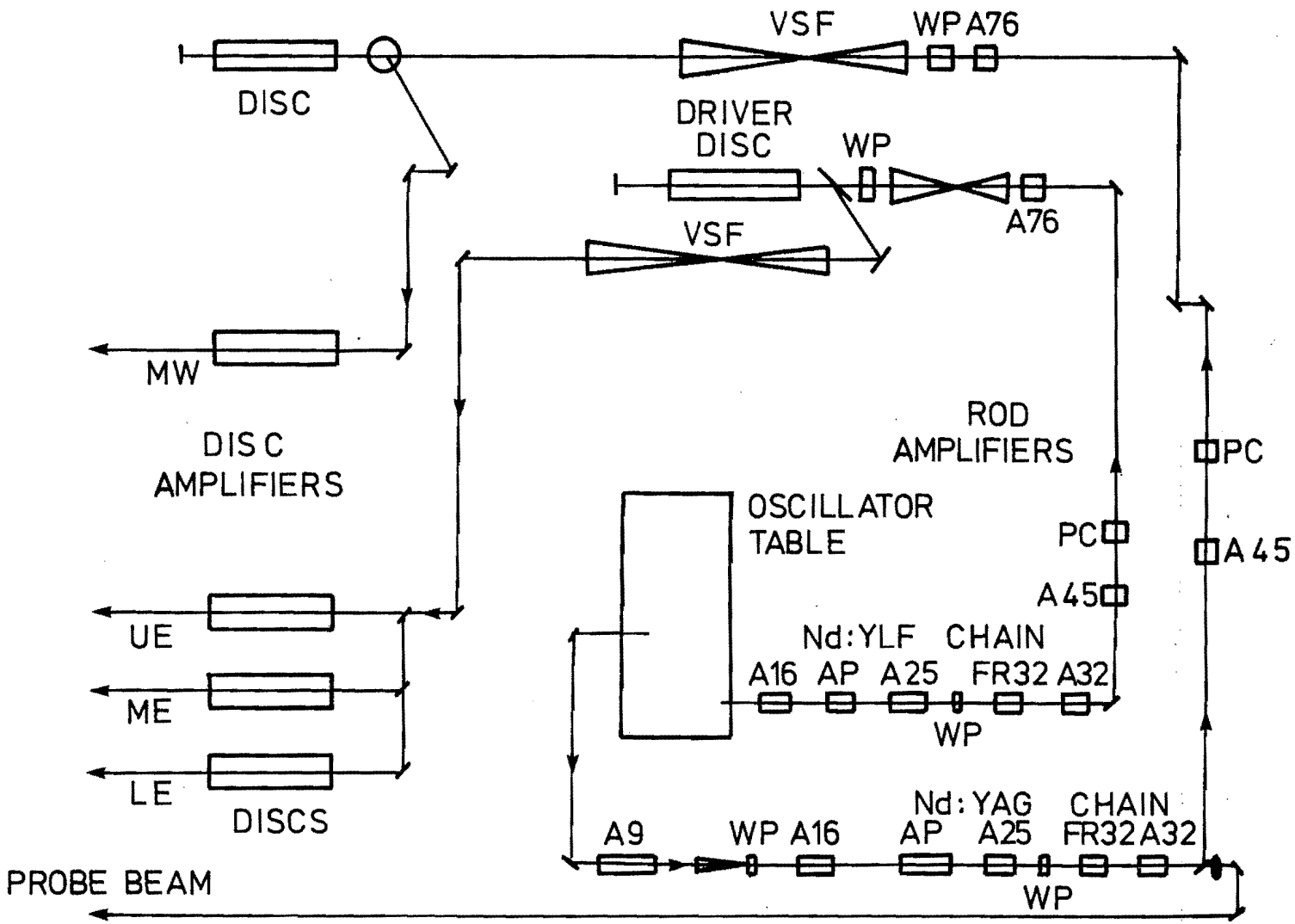

VULCAN CONFIGURATION FOR SEPERATE PROPAGATION
FIGURE 20

one of the Beat-wave interaction pulses and two probe pulses.

The system modifications for the 1.064 micron amplifier chain included the installation of mirrors to inject the pulse into the normal 'short pulse' amplifier chain and changing the pre-amplifier from Nd:YLF operation to Nd:YAG operation. As previously, the extra 9 mm diameter amplifier was installed, although it was possible to operate it with phosphate for these experiments eliminating the problems encountered with the previous system design. Mirrors were installed to direct the beams through the appropriate output disc amplifiers. With these system modifications it was possible to amplify the pulses to the required energies.

Efficient Beam Combining

To combine the two wavelengths efficiently at the output of the system a novel system was adopted as shown in Figure 21. The two beams, orthogonally polarised, are incident on a polariser as shown. A wave-plate was designed such that it provided full wave retardation at 1.064 microns and half-wave retardation at 1.053 microns. Accurate calculations were made to calculate the optimum thickness of a suitable quartz retarder. The phase difference, ϕ, of the e and o ray of a single wavelength, λ, passing through a waveplate of thickness, t, is given by

$$\phi = 2\pi t\,(n_e - n_o)/\lambda \qquad 4.9$$

where n_e and n_o are the refractive indices of the e and o ray respectively. To generate a π phase shift between the two wavelengths, λ_1 and λ_2, therefore

$$\phi_1 - \phi_2 = \pi = 2\pi t\,((n_e - n_o)/\lambda_1 - (n_e - n_o)/\lambda_2) \qquad 4.10$$

Using appropriate values of refractive index (4.5) a value of t can be calculated at

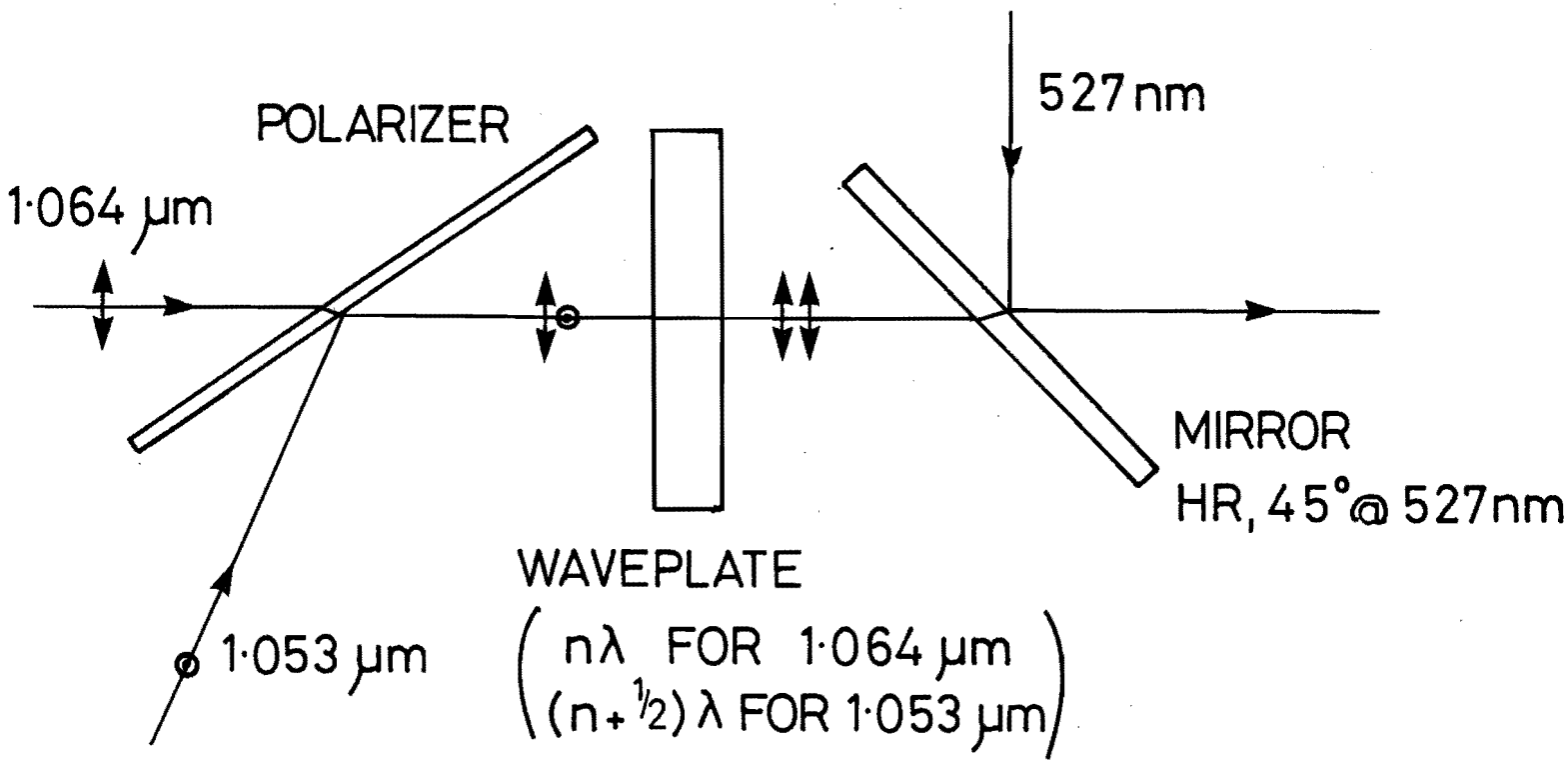

TWO WAVELENGTH COMBINING IN THE TARGET AREA
FIGURE 21

5.46 mm. This thickness produces a 90 degree difference in polarisation but does not generate a half or full phase shift at either wavelength. The thickness of the phase-plate was therefore set to the nearest number of full wave cycles at 1.064 microns, 45, giving a retardation at 1.053 microns of 180.37 degrees, ie a retardation accuracy of better than 0.25%.

The two output beams on target were in the same polarisation giving an 88% combination efficiency. If only mirrors had been used to combine the beams it would only have been possible to achieve 50% efficiency. The introduction of the 527nm beam, shown in Figure 21, was to photo-ionise the plasma.

This system of combining the beams was found to work well. One problem that did arise was a decrease in its efficiency due to optical damage to the polariser. Once the polariser was replaced the combining efficiency returned to greater than 80%.

CONCLUSION

To generate the required pulses for the Beat-wave experiment two different oscillator systems were developed. The first housed the two lasing media in the same cavity. This oscillator successfully demonstrated that the Vulcan configuration designed to amplify the two pulses to the required energies would work in an experiment, but problems with optical output stability required a second oscillator system to be designed.

The second oscillator system housed the two lasing media in separate optical cavities. Their outputs were synchronised by careful control of the Q-switching and mode-locking electronics. This system has been shown to work reliably during three scheduled Beat-wave experiments.

The Vulcan amplification system was redesigned in order to amplify the pulses to the high output energies required. For the December 1985 experiment the two pulses were propagated along a common amplifier path. To achieve similiar output energies of the two pulses two amplifying media were required; neodymium doped phosphate and silicate glasses, which preferentially amplify the two wavelengths. As the two amplified pulses propagated through the atmosphere side-bands were generated due to Raman Scattering in nitrogen (4.4). This effect was detrimental to observing the presence of a Beat-wave, therefore it was necessary to redesign the Vulcan amplifier configuration.

The new arrangement propagated the two pulses in separate amplifier chains. To combine the two beams efficiently a novel system was designed using a polariser and a multi-order waveplate. The new amplifier configuration and beam combiner was used in two Beat-wave experiments and were both found to work well.

The experiment in May 1987 (5.2) showed that side-band generation was still a problem as the beam passed through the waveplate in the beam combiner (5.3). For the experiment in August 1988 an alternative diagnosis technique was therefore adapted to monitor the presence of the Beat-wave (5.4). This allowed the first

demonstration of the existence of a Beat-wave generated using one micron radiation (5.5).

The oscillator and sytem development described in this thesis has been presented at a number of conferences (5.6, 5.7, 5.8, 5.9) and has also been summarised in the Annual Report to the Laser Facility Committee within the SERC (5.10, 5.11).

The work presented in this thesis has played a decisive role in the plasma Beat-wave program at the Rutherford Appleton Laboratory. The developments described and the susequent experiments performed at the laboratory have resulted in a proposal to the EEC, subsequently funded, to provide support for a joint European program on Beat-wave studies.

REFERENCES

CHAPTER 1

1.1 Bertolotti, Masers and Lasers, p.115. Adam Hilger Ltd., 1983.

1.2 RH Dicke, US Patent 2,581,652. Sept 9, 1958.

1.3 AL Schawlow and CH Townes, Phys Rev, Vol 112, p.1940. 1958.

1.4 A Javan, Phys Rev Lett, Vol 3. No 2, p.87. July 15, 1959.

1.5 JH Sanders, Phys Rev Lett, Vol 3, No 2, p.87. July 15, 1959.

1.6 TH Maiman, Nature, No 4736, p.493. Aug 6, 1960.

1.7 A Javan et al, Phys Rev Lett, Vol 6, p.106. 1961.

1.8 CKN Patel, Phys Rev, Vol 136, No 5A, p.1187. Nov 30, 1964.

1.9 LF Johnson and K Nassau, Proc IRE, Vol 49, p.1704. 1961.

1.10 E Snitzer, Phys Rev Lett, Vol 7, No 12, p.444. Dec 15, 1961.

1.11 JE Geusic et al, App Phys Lett, Vol 4, p.182. 1964.

1.12 Kisliuk and Boyd, Proc IRE, Vol 49, p.1635. 1961.

1.13 FJ McClung and RW Hellwarth, Proc of the IEEE, p.46. Jan 1963.

1.14 LE Hargrove et al, App Phys Lett, Vol 5, No 1, p.4. 1 July, 1963.

1.15 T Deutsch, App Phys Lett, Vol 7, No 4, p.80. 15 July, 1965.

1.16 Laser and Applications, Laser Pioneer Interviews, High Tech Productions Ltd., Dec 1985.

1.17 W Koechner, Solid State Laser Engineering, 2nd Edition, Springer Series in Optical Sciences, No 1. 1988.

CHAPTER 2

2.1 T Tajima and JM Dawson, Phys Rev Lett, Vol 43, p.267. 1979.

2.2 CE Clayton et al, Phys Rev Lett, Vol 54, No 21, p.2343. 1985.

2.3 N Ebrahim et al, Proc 1986 Linear Accelerator Conf., Stanford, Ca.

2.4 RG Evans, RAL, Private communication, Feb 1990.

CHAPTER 3

3.1 DJ Kuizenga and AE Siegman, IEEE J of QE, Vol 6, p.694. Nov 1970.

3.2 W Koechner, Solid State Laser Engineering, 2nd Edition, Chapter 8, p.434.

3.3 W Koechner, Solid State Laser Engineering, 2nd Edition, Chapter 3, p.101.

3.4 J Marling, IEEE J of QE, Vol 14, p.56. 1978.

3.5 JE Murray, IEEE J of QE, Vol 19, No 4, p.488. April 1983.

CHAPTER 4

4.1 Lawrence Livermore National Laboratory, Laser Program Annual Report - 1976, p.2-62.

4.2 LM Frantz and JS Nordvik, J of Appl Phys, Vol 34, No 8, p.2346. Aug 1963.

4.3 W Koechner, Solid State Laser Engineering, 2nd Edition, Chapter 4, p.133.

4.4 AE Dangor et al, J Phys B, Vol 22, p.797. 1989.

4.5 Private Communication from G Jones, Gooch and Housego Ltd. 1988.

CHAPTER 5

5.1 AE Dangor et al, IEEE Trans on Plasma Sci, Vol PS-15, No 2. April 1987.

5.2 T Garvey et al, From High Brightness Accelerators, Plenum Publishing Corp. 1988.

5.3 A Dyson et al, J Phys B, Vol 22, p.231. 1989.

5.4 AE Dangor et al, J Appl Phys, Vol 64, No 11. 1 Dec 1988.

5.5 A Dyson et al, To be published but also appears in RAL Report 89-045.

5.6 CN Danson, CB Edwards and IN Ross, Presented at CLEO'85, Baltimore,

USA.

5.7 CN Danson et al, Presented at QE-VII, Malvern. Sept 1985.

5.8 CN Danson et al, Invited paper at the 1st International Laser Science Conference, Dallas, Texas. Nov 1985.

5.9 CN Danson et al, Presented at QE-VIII, St. Andrews. Sept 1987.

5.10 CN Danson, CB Edwards and RW Wyatt. Annual Report to the Laser Facility Committee, RAL-86-046, Section C1.1. 1986.

5.11 CN Danson, CB Edwards, D Rodkiss and R Wyatt. Annual Report to the Laser facility Committee, RAL-86-046, Section C1.2. 1986.